

Tau Neutrino Physics in km³ Detectors

Ina Šarčević

University of Arizona

ina@physics.arizona.edu

- Astrophysical Sources of Ultra-High Energy Neutrinos
- Studying $\nu_\mu \rightarrow \nu_\tau$ Oscillations with 1000 Megaparsec Baseline
- Distinctive Energy and Nadir Angle Dependence of the Upward ν_τ Flux
- Detection of Tau Neutrinos with km³ Detectors
- Ultrahigh Energy Neutrinos as Probes of New Physics

- Since neutrinos are highly stable, neutral particles cosmic neutrinos point back to astrophysical point sources and bring information from processes otherwise obscured by a few hundred gm of a material.

- Interaction length of a neutrino is

$$\mathcal{L}_{\text{int}} \equiv \frac{1}{\sigma \cdot N_A}$$

Interaction length of 1TeV neutrino is 250 kt/cm² or column of water of 2.5 million km deep.

- Neutrino astronomy could provide a unique window into the deepest interiors of stars and galaxies, while HE photons get absorbed by a few hundred gm of a material.
- UHE Neutrinos could also provide unique probe of physics beyond the Standard Model.

Sources of UHE Neutrinos

- **Cosmogenic Neutrinos**

Neutrinos produced by high energy cosmic rays interacting with the microwave background radiation (photoproduction followed by pion decay).

- **Neutrinos from AGNs**

AGNs are believed to be prodigious particle accelerators and the most powerful radiation sources known in the Universe, with luminosities ranging from 10^{42} – 10^{48} erg/s. If the observed TeV gamma rays (from **Mkn 421** and **Mkn 501**) originate in the decay of π^0 , then AGNs may also be the most powerful sources of UHE neutrinos.

- **Neutrinos from GRBs**

The cosmological GRB fireball energy is expected to be converted by photo-meson production to a burst of high energy neutrinos.

- **Neutrinos from Topological Defects**

Topological Defects formed in the Early Universe are believed to be non-accelerator sources of UHE neutrinos. In the TD models neutrinos are produced directly at UHEs by the cascades initiated by the decay of a supermassive elementary "X" particle associated with some Grand Unified Theory (GUT), rather than being accelerated. The X particle are usually thought to be released from topological monopoles left over from GUT phase transition and it decays into quarks, gluons, leptons.

- It seems plausible that protons generated within an AGN interact with matter or radiation in the AGN disk, or with UV photons in the associated jets, to produce pions whose decay products include PHOTONS and NEUTRINOS

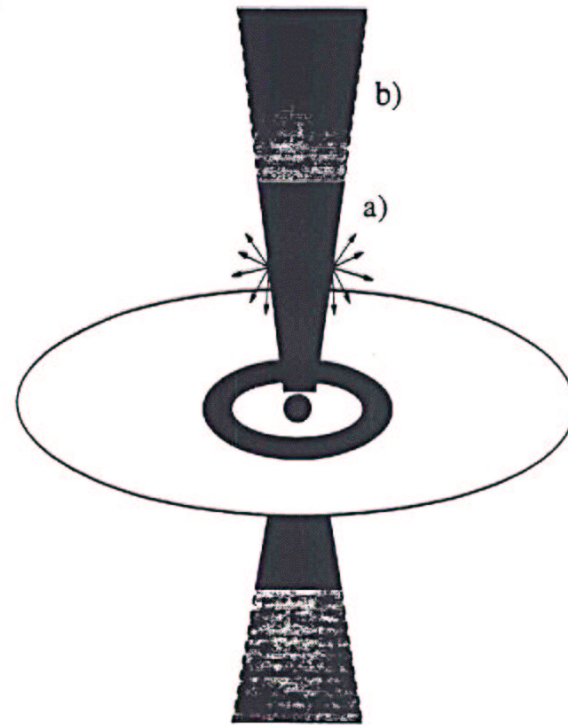


FIG. 1. Schematic diagram of the central engine of an AGN (not to scale). A supermassive black hole at the center is surrounded by an accretion disk of gas falling into the black hole. Two jets of plasma are ejected perpendicular to the disk. Typically, shocks form in the jets. In such shocks (wavy line), protons are accelerated, which eventually leave the jet and drift back to the disk. In the inner region (dark ring, $\approx 10R_S$ to $\approx 200R_S$), protons reaching the disk initiate cascades through $p\gamma$ interactions. Only protons accelerated in the outer region (b) of the jet can reach energies above the threshold for $p\gamma$ reactions with UV photons.

- The observed photon energy spectrum is a power-law:

$$\frac{dN_\gamma}{dE_\gamma} \approx E_\gamma^{-2}$$

for $100\text{MeV} \leq E_\gamma \leq 2\text{TeV}$

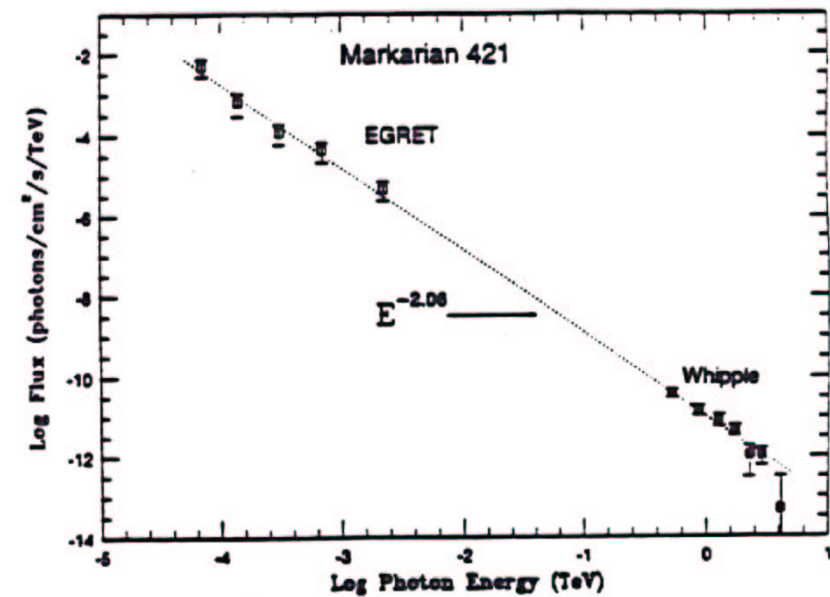
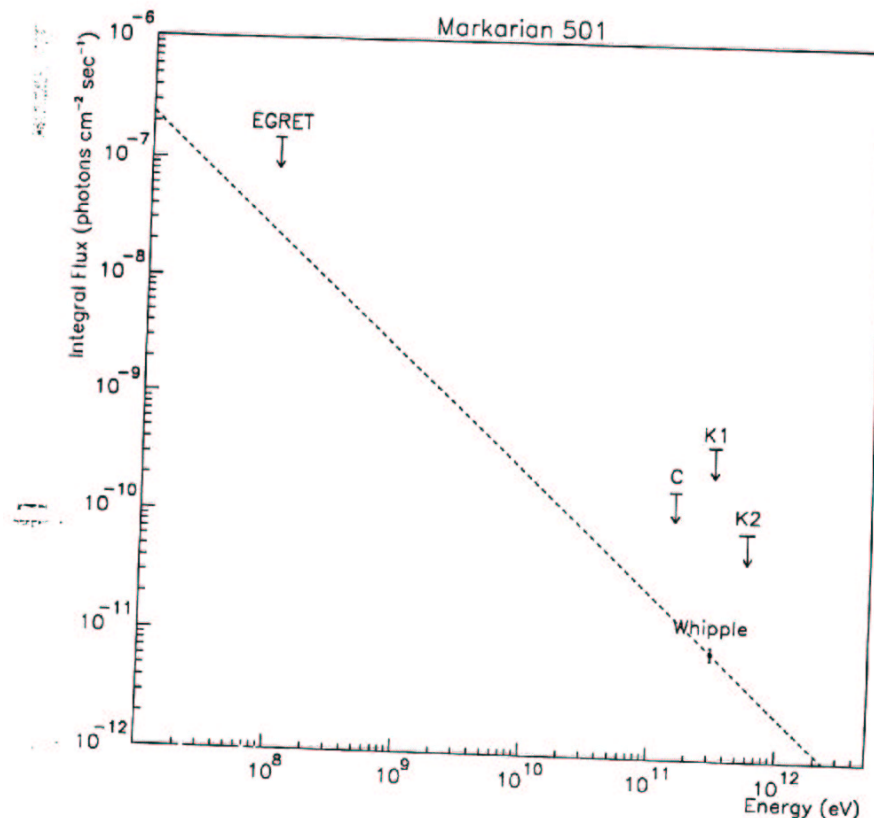


Figure 2. Differential energy spectrum from both the EGRET (Lin et al. 1992) and Whipple observations of Markarian 421. The EGRET observations were taken 27 June - 11 July, 1991; the Whipple observations 24 March - 2 June 1992. A single power-law, with energy exponent 2.06 ± 0.04 , is an acceptable description of the combined dataset. Possible systematic errors in the exponents are not included. They are difficult to estimate because of the differing technique by which the fluxes have been measured and because of the non-contemporaneous nature of the observations.

Courtesy of T.C. Weekes (Whipple)



T.C. Weekes (Whipple)

Table 1.

Nearby Bl Lac Objects (out to $z = 0.11$).

Object	Alias	z	EGRET ($10^{-7} \text{cm}^{-2} \text{s}^{-1}$)	FLWO 100 MeV	Alpha 300 GeV	OX/ Alpha RO
1101+384	Mrk421	0.031	1.4 ± 0.4	Detected		1.14/0.42
1652+398	Mrk501	0.034	<1.5	Detected		1.15/0.48
1ES2344+514		0.044	?	Detection?		1.18/0.41 ApJ 50P (9*)
1113+704	Mrk 180	0.046	<0.4	Upper limit		1.27/0.35
1ES1959+650		0.048	?	Upper limit		1.19/0.32
1514-241	Ap Lib	0.049	<1.0	S.H.		
1807+698	3C371	0.050	<0.9	Upper limit		1.72/0.50
0521-365	PKS	0.055	1.8 ± 0.5	S.H.		
1727+502	I Zw 187	0.055	<0.8	Upper limit		1.01/0.47
1ES2321+419		0.059	?	Upper limit		1.19/0.32
0548-322	PKS	0.069	<1.0	S.H.		1.02/0.39
2200+420	B1 Lac	0.069	Detected	Upper limit		1.31/0.61
2005-489	PKS	0.071	1.8 ± 0.5	S.H.		1.11/0.53
1ES1741+196		0.083	?	Not yet observed		1.18/0.41
1219+285	W COM	0.102	0.8 ± 0.2	Upper limit		1.27/0.61

Sky & Telescope (1992)

ACTIVE GALACTIC NUCLEI: SORTING OUT THE MESS

BY ANN FINKBEINER

MOST GALAXIES are bright in their centers, but decorously so. "Active" galaxies, on the other hand, have centers that are immodestly bright. Dazzling light from a tiny nucleus all but swamps the rest of the galaxy. In fact active galactic nuclei, or AGNs as they are called, are the brightest things in the universe.

AGNs come in a bewildering variety of forms. In recent years, however, our picture of them has been growing simpler and clearer, just as their role in the cosmos is assuming new importance.

Only about one percent of galaxies have active nuclei. But over the history of the universe, these objects have produced nearly as much energy as all galaxies combined. And, strangely, most of that bright light cannot be coming from stars. Stars give off most of their energy in a rather narrow range of wavelengths, from mid-ultraviolet to mid-infrared, but AGNs shine across the entire spectrum, from radio to gamma-ray wavelengths. Whatever is lighting them up is not what lights up most of the rest of the universe.

Other properties of AGNs are equally extreme. They change brightness substantially on all time-scales from minutes to at least decades. Some send out spectacular squirts of gas millions of light-years long. A few are relatively close by, but most (including the extremely luminous ones) inhabit the distant and early universe; they were far more common then than they are now. In fact AGNs are the earliest congregations of matter known — the visible

Only about one percent of galaxies have active nuclei. But over the history of the universe, these objects have produced nearly as much energy as all galaxies combined.

signs of the first systems to coalesce after the Big Bang.

Since the early 1940s astronomers have been collecting these extravagant characters and classifying them under various names: Seyfert 1 and Seyfert 2 galaxies, broad-line and narrow-line radio galaxies, radio-loud and radio-quiet quasars, optically violent variable quasars, and BL Lacertae objects. Until recently, however, astronomers hadn't much sense of whether the different types of AGNs were related, what they were, or how they worked. "We had been doing botany," says C. Megan Urry, an astronomer at the Space Telescope Science Institute who specializes in active galaxies, "and now we're undoing that mess."

Undoing the mess means astronomers now more or less agree that all AGNs are different aspects of the same phenomenon. The theory is simple: AGNs look different only because we see the same type of object tilted at different angles on the sky. Astronomers also agree that the power source underlying them all is probably a supermassive black hole violently sucking in quantities of gas. The relatively tiny black hole and its hot surroundings lie within a large, thick torus, a doughnut of dust and cooler gas. This in turn is surrounded on all sides by larger cooler gas clouds spaced widely apart. The whole affair forms the nucleus of a galaxy.

There's no agreement yet on exactly how the AGN phenomenon works. But if astronomers are right about what AGNs are and once they figure out how AGNs function, these exaggerated objects might provide crucial evidence about the beginning and innermost workings of all galaxies.

THE FIRST SIGNS

AGN collecting began 50 years ago when Rudolph Minkowski and Milton Humason at Mount Wilson Observatory handed over the spectra of several spiral galaxies with oddly bright centers to a postdoctoral student, Carl K. Seyfert. Spectra are little rainbows of an object's light spread out to display all its colors, or wavelengths. An astronomical object's spectrum is usually marked by many thin bright or dark lines that reveal volumes about conditions in and around the light source. Bright lines come from tenuous hot gas, dark ones from cooler gas through which the light passes. Usually the spectral lines are very thin, but sometimes they are broadened because the gas is especially hot or moving rapidly.

Normally the spectra of spiral galaxies

Gamma Ray Bursts (GRBs)

Fireball Model: GRB are produced by the dissipation of the kinetic energy of the relativistic expanding fireball with a large fraction ($> 10\%$) of foreball energy being converted by photopion production to HE neutrinos. HE protons accelerated in ultrarelativistic shocks interact with synchrotron photons inside the fireball.

$$F_{\nu+\bar{\nu}}^s(E) = 4.0 \times 10^{-\alpha} E^{-n},$$

where $\alpha = 13$ and $n = 1$ for $E < 10^5$ GeV and $\alpha = 8$, $n = 2$ for $10^5 < E < 10^7$ GeV and $n = 3$ for $E > 10^7$ GeV.

Waxman-Bahcall, *Phys. Rev. D* 59, 023002 (1999)

Recently another mechanism was proposed for producing TeV neutrinos with predicted neutrino flux given by:

$$F_{\nu+\bar{\nu}}^s(E) = 10^{-7} E^{-2}$$

Meszaros and Waxman, *Phys. Rev. Lett.* 87, 171102 (2001)

Neutrinos from Topological Defects

- Topological defects: monopoles, cosmic strings, domain walls, and superconducting cosmic strings, might have been formed in symmetry-breaking phase transitions in the early Universe.
 - * In the so-called "top-down" (TD) models, γ -rays, electrons (positrons), and neutrinos are produced directly at UHEs by the cascades initiated by the decay of a supermassive elementary "X" particle associated with some Grand Unified Theory (GUT), rather than being accelerated (i.e. TD might constitute a "nonacceleration" source of UHE neutrinos). The X particle are usually thought to be released from topological monopoles left over from GUT phase transition and it decays into quarks, gluons, leptons.
- Predicted spectra are much harder and extend much further beyond 100EeV than shock acceleration spectra.
- TD might be responsible for the highest energy events observed ($E \sim 10^{21}$ eV) → Fly's Eye and AGASA Experiments (Fig.)

Topological Defect Models:

Sigl-Lee-Schramm-Coppi (SLSC)

Wichoski-MacGibbon-Brandenberger (WMB)

- Energy loss of the string network converted into gravitational radiation or particle production
- Upper limits from cosmic ray data (Frejus, Fly's Eye)
- Upper limit for strong source evolution

$$2 \times 10^{-8} E^{-2}$$

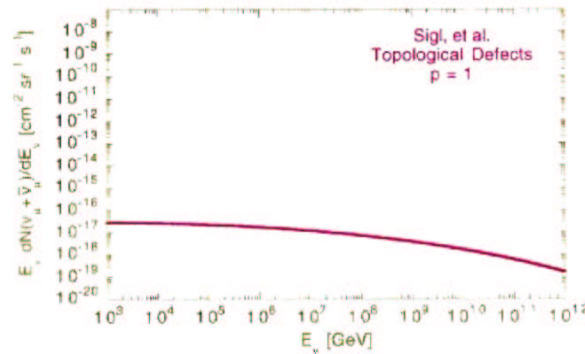
Non-acceleration Sources

Topological Defects $\rightarrow X \rightarrow \dots \rightarrow \nu + \dots$

Rate of release of X particles is

$$\frac{dN_X(t)}{dt} = \kappa M_X^p t^{-4+p}$$

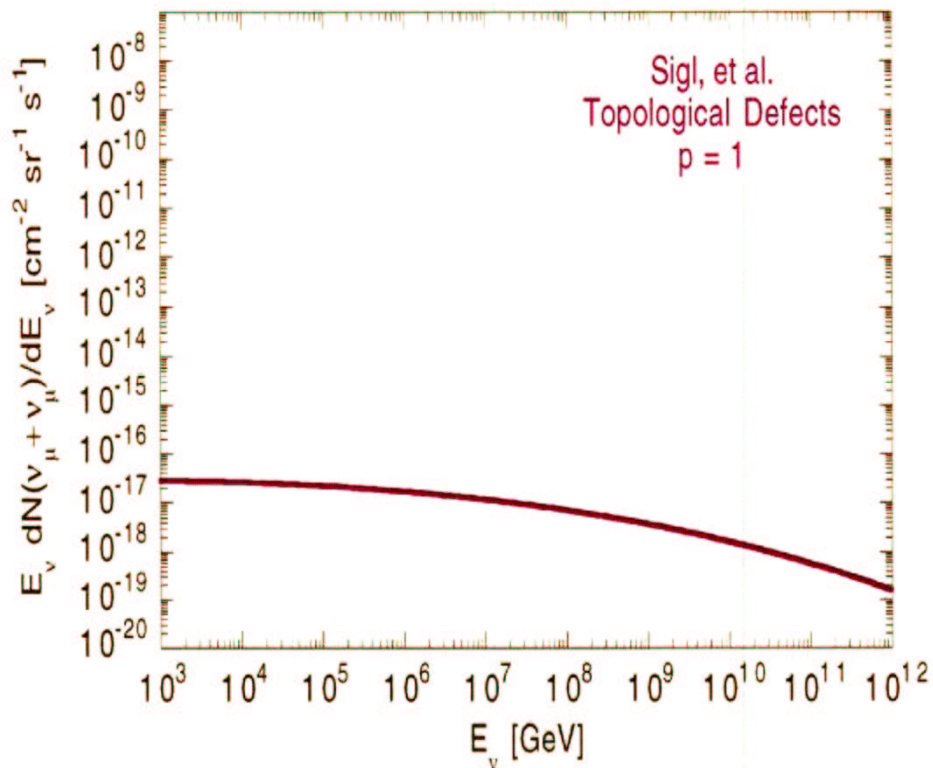
$p = 1$: collapse of cosmic-string loops

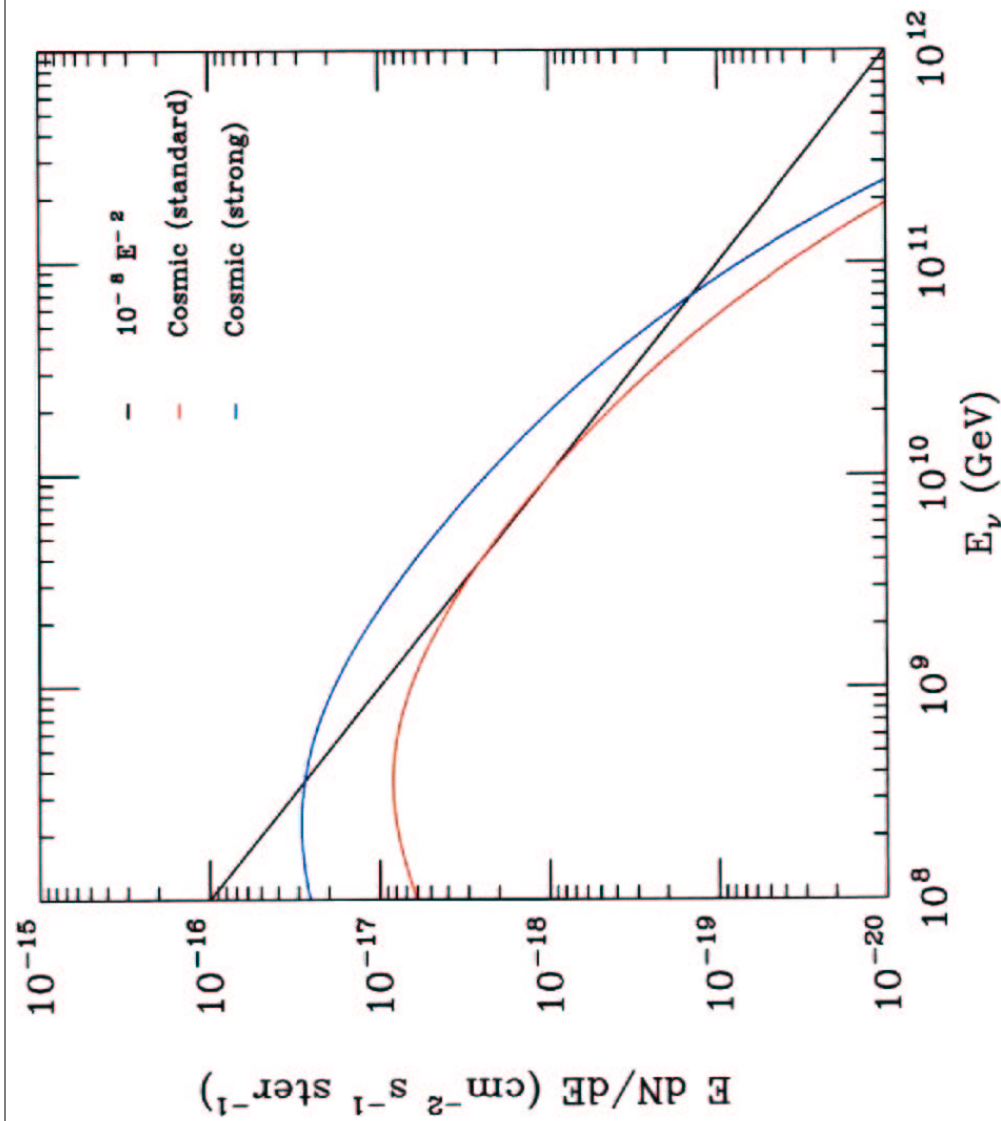
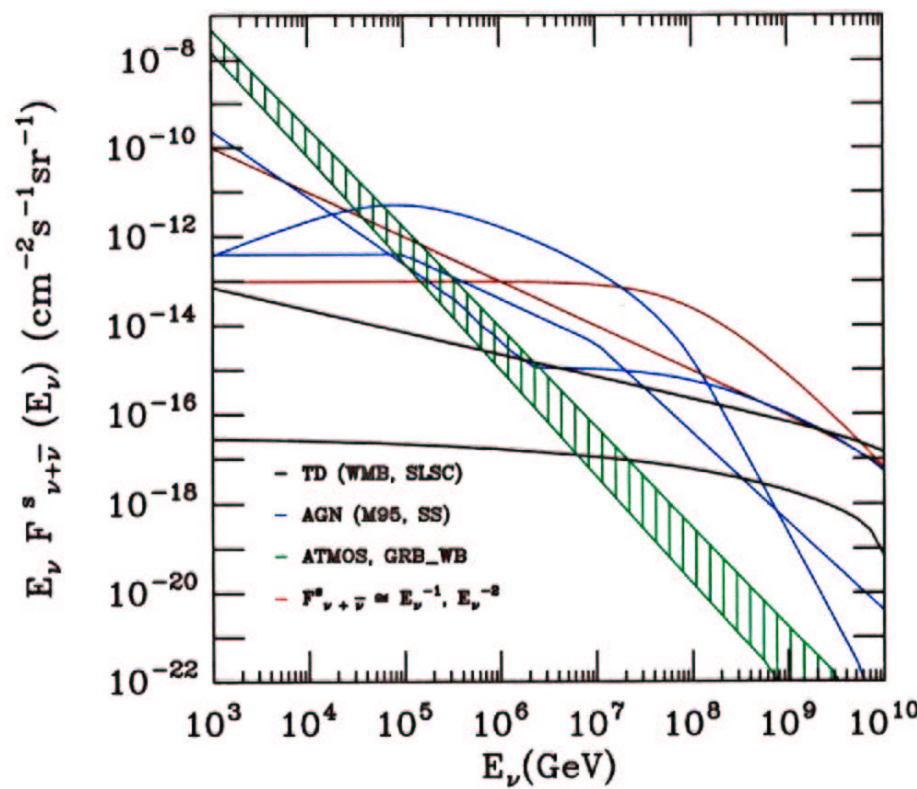


$\lesssim 0.1$ downward event/yr/km³, $E_\mu^{\min} = 10^7$ GeV.

(Comparable to rates expected from CR-4 cosmic ν flux.)

G. Sigl, et al., *Phys. Lett. B* **392**, 129 (1997)





- Basic processes of neutrino production in extragalactic sources

$$p + \gamma \rightarrow n + \pi^+$$

$$\hookrightarrow n + \gamma \rightarrow p + \pi^-$$

$$\hookrightarrow \pi^+ \rightarrow \mu^\pm + \nu_\mu$$

$$\hookrightarrow \mu^\pm \rightarrow e^\pm + \nu_\mu + \nu_e$$

$$p + \gamma \rightarrow p + \pi^0$$

$$\hookrightarrow \pi^0 \rightarrow \gamma\gamma$$

- For astronomical distances, i.e. $L \sim 1000 Mpc$

$$\langle \sin^2\left(\frac{1.27\Delta m^2 L(Km)}{E(GeV)}\right) \rangle = \frac{1}{2}$$

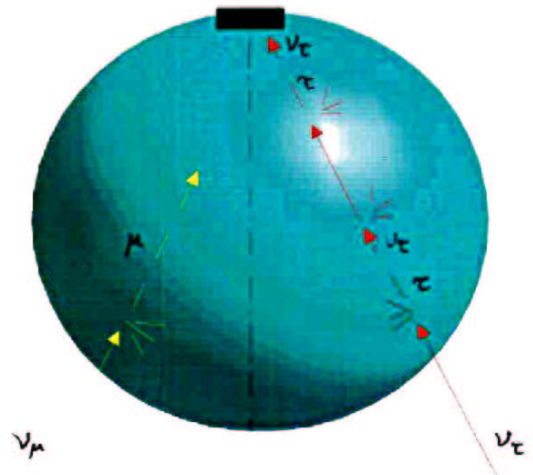
(For PeV neutrinos potentially sensitive to $\Delta m^2 \sim 10^{-17} \text{eV}^2$!)

- Thus, for large mixing angle, the probability for $\nu_\mu \rightarrow \nu_\tau$ oscillations given by

$$P(\nu_\mu \rightarrow \nu_\tau; L) = \sin^2 2\theta \sin^2\left(\frac{1.27\Delta m^2 L(Km)}{E(GeV)}\right)$$

becomes 1/2, i.e.

$$F_{\nu_\mu} = F_{\nu_\tau}$$



- Qualitative behavior of ν_τ is different than ν_μ in propagation through Earth

(Halzen and Saltzberg, PRL 81 (1998))

- As ν_μ 's propagate through the Earth, their flux get attenuated while ν_τ 's get regenerated via τ decay

$$\nu_\mu + N \rightarrow \mu + X$$

and muons get absorbed, while

$$\nu_\tau + N \rightarrow \tau + X$$

followed by the τ decaying back into ν_τ

$$\tau \rightarrow \nu_\tau + X$$

(muon lifetime: $\tau_\mu = 2.2 \times 10^{-6} s$)

(tau lifetime: $\tau_\tau = 2.9 \times 10^{-13} s$)

tau decay length:

$$\rho_\tau^{dec}(E, X) = \gamma \tau_\tau \rho(X)$$

- Tau charged-current interaction length and the photonuclear interaction length become comparable to the tau decay length at $E > 10^8$ GeV

- Main difference due to lifetimes:

$$\tau_\mu = 2.2 \times 10^{-6} s$$

$$\tau_\tau = 2.9 \times 10^{-13} s$$

ν_μ Propagation through the Earth

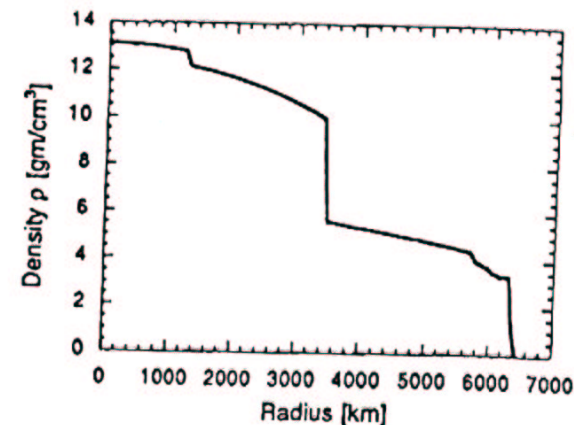
- Transport equation for ν_μ

$$\frac{\partial F_{\nu_\mu}(E, X)}{\partial X} = -\frac{F_{\nu_\mu}(E, X)}{\lambda_{\nu_\mu}(E)} + \int_E^\infty dE_y \left[\frac{F_{\nu_\mu}(E_y, X)}{\lambda_{\nu_\mu}(E_y)} \right] \frac{dn^{NC}}{dE}(E_y, E)$$

where X is the column depth,

$$X = \int_0^L \rho(L') dL'$$

- Density Profile of the Earth



Preliminary Earth Model

- We assume solution of the form:

$$F_\nu(E, X) = F_\nu^0(E) \exp \left[-\frac{X}{\Lambda_\nu(E, X)} \right]$$

$$\Lambda_\nu(E, X) = \frac{\lambda_\nu(E)}{1 - Z(E, X)}$$

where Z-moments are

$$Z = Z_\nu + Z_\tau$$

$$Z_\tau = \left[\frac{1}{X} \right] \int_0^X \int_0^1 \frac{\lambda_\nu(E)}{\rho_\tau^{dec}(E, \theta)} \Phi_\nu^{dec}(y, E) \eta_\nu(y, E)$$

$$\times \exp \left[-\frac{X'}{\Lambda_\nu(E_y, X')} \right] \frac{F_\tau(E_y, X')}{F_\nu^0(E_y)} dX' dy.$$

ν_τ Propagation through the Earth

- Coupled transport equations for the flux of ν_τ and τ :

$$\begin{aligned} \frac{\partial F_{\nu_\tau}(E, X)}{\partial X} = & -\frac{F_{\nu_\tau}(E, X)}{\lambda_{\nu_\tau}(E)} + \int_E^\infty dE_y \left[\frac{F_{\nu_\tau}(E_y, X)}{\lambda_{\nu_\tau}(E_y)} \right] \frac{dn^{NC}}{dE}(E_y, E) \\ & + \int_E^\infty dE_y \left[\frac{F_\tau(E_y, X)}{\rho_\tau^{dec}(E_y)} \right] \frac{dn^{dec}}{dE}(E_y, E) + \int_E^\infty dE_y \left[\frac{F_\tau(E_y, X)}{\lambda_\tau(E_y)} \right] \frac{dn^{CC}}{dE}(E_y, E) \end{aligned}$$

and for the τ 's

$$\begin{aligned} \frac{\partial F_\tau(E, X)}{\partial X} = & -\frac{F_\tau(E, X)}{\lambda_\tau(E)} - \frac{F_\tau(E, X)}{\rho_\tau^{dec}(E, X, \theta)} \\ & + \int_E^\infty dE_y \left[\frac{F_{\nu_\tau}(E_y, X)}{\lambda_{\nu_\tau}(E_y)} \right] \frac{dn^{CC}}{dE}(E_y, E) + \int_E^\infty dE_y \left[\frac{F_\tau(E_y, X)}{\lambda_\tau(E_y)} \right] \frac{dn^{\tau\tau}}{dE}(E_y, E) \end{aligned}$$

- We include all τ decay modes with corresponding branching fraction and energy distribution

$$\tau \rightarrow \nu_\tau \mu \nu_\mu \dots \dots B_\tau = 0.36$$

$$\tau \rightarrow \nu_\tau e \nu_e \dots \dots B_\tau = 0.12$$

$$\tau \rightarrow \nu_\tau \rho \dots \dots B_\tau = 0.26$$

$$\tau \rightarrow \nu_\tau a_1 \dots \dots B_\tau = 0.13$$

- We assume solution of the form:

$$F_\nu(E, X) = F_\nu^0(E) \exp \left[-\frac{X}{\Lambda_\nu(E, X)} \right]$$

$$\Lambda_\nu(E, X) = \frac{\lambda_\nu(E)}{1 - Z_\nu(E, X)}$$

where Z-moments are defined as

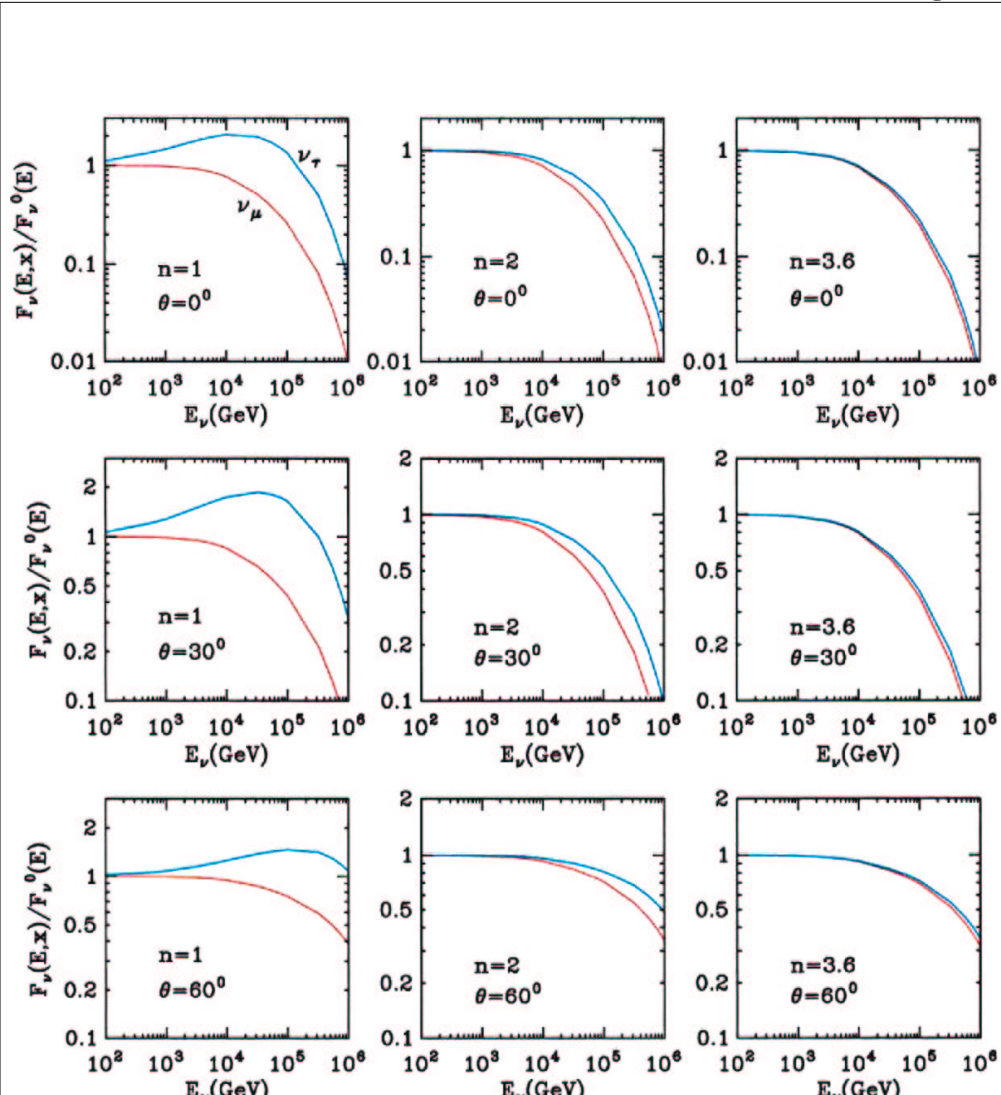
$$Z_\nu(E, X) = \int_0^1 \eta_\nu(y, E) \Phi_\nu^{nc}(y, E) \left[\frac{1 - e^{-XD_\nu(E, E_y, X)}}{XD_\nu(E, E_y, X)} \right] dy,$$

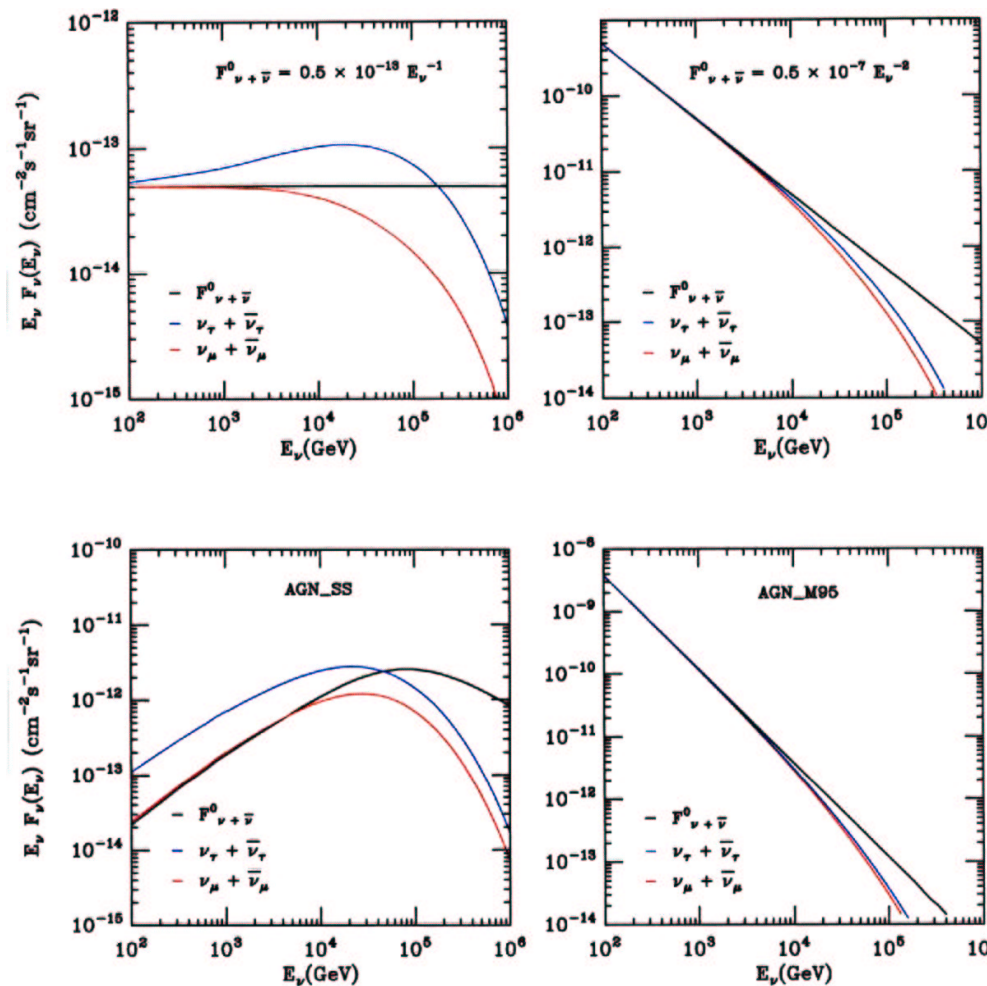
and

$$D_\nu(E, E_y, X) = \frac{1}{\Lambda_\nu(E_y, X)} - \frac{1}{\Lambda_\nu(E, X)}$$

$$\eta_\nu(y, E) = \frac{F_\nu^0(E_y)}{F_\nu^0(E)(1-y)}$$

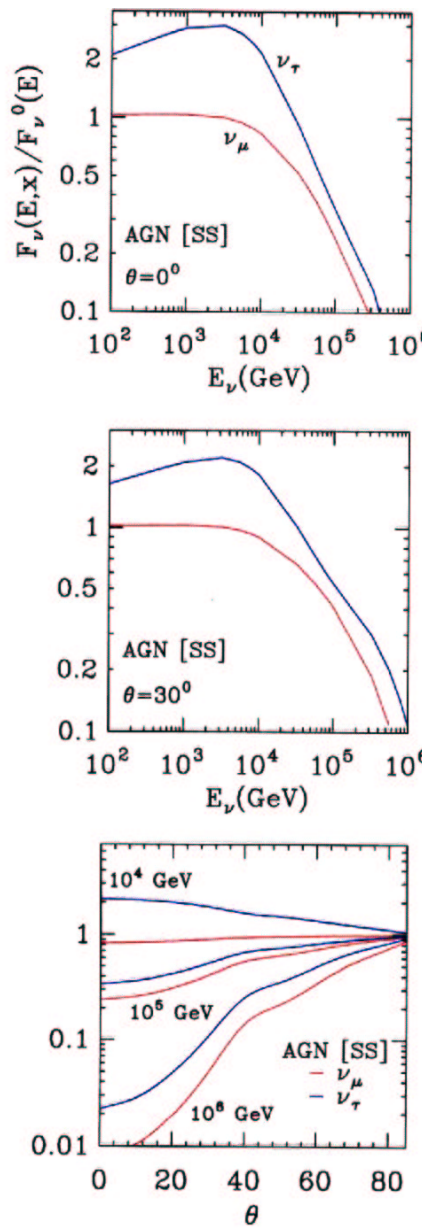
$$\frac{d\sigma_{\nu N \rightarrow \nu X}(y, E_y)}{dy} = \Phi_\nu^{nc}(y, E) \sigma_{\nu N}^{tot}(E)$$





Tau Neutrino Detection

- *Upward Muons*
 - signal : $\nu_\tau N \rightarrow \tau X$
 $\leftrightarrow \tau \rightarrow \nu_\tau \nu_\mu \mu$
 - background : $\nu_\mu N \rightarrow \mu X$
- *Upward Hadronic/Electromagnetic Showers*
 - signal : $\nu_\tau N \rightarrow \tau X$
 $\tau \rightarrow \nu_\tau X/e$
 - background : $\nu_{\mu,e} N \rightarrow \nu_{\mu,e} X$
 $\nu_e N \rightarrow e X$



Signal

- Upward muons from ν_τ interactions:

$$R_{\nu_\tau} = A N_A \int_{E_\mu^{min}}^{\infty} dE_\nu / dy / dz < R(E_\nu(1-y)z, E_\mu^{min}) >$$

$$\times \frac{dn(E_\nu(1-y)z) d\sigma_{cc}(E_\nu, y)}{dz} F_\nu(E_\nu, X) \Theta(E_\nu(1-y)z - E_\mu^{min})$$

- Decay distribution for τ : $\frac{dn(E_\tau)}{dz}$
- Branching fraction for $\tau \rightarrow \nu_\tau \nu_\mu \textcolor{red}{\nu}_e$: 0.18
- Area : $1Km^2$

Background

- *Upward muons from ν_μ interactions:*

$$R_{\nu_\mu} = A N_A \int_{E_\mu^{min}}^{\infty} dE_\nu \int dy < R(E_\nu(1-y), E_\mu^{min}) >$$

$$\times \frac{d\sigma_{cc}(E_\nu, y)}{dy} F_\nu(E_\nu, X) \Theta(E_\nu(1-y) - E_\mu^{min})$$

- **Neutrino energy loss :** $y = \frac{E_\nu - E_\mu}{E_\nu}$
- **Upward neutrino flux :** $F_\nu(E_\nu, X)$
- **CC differential cross section :** $\frac{d\sigma_{cc}(E_\nu, y)}{dy}$
- **Average range of muon :** $< R(E_\mu, E_\mu^{min}) >$
 - **Area :** $1Km^2$

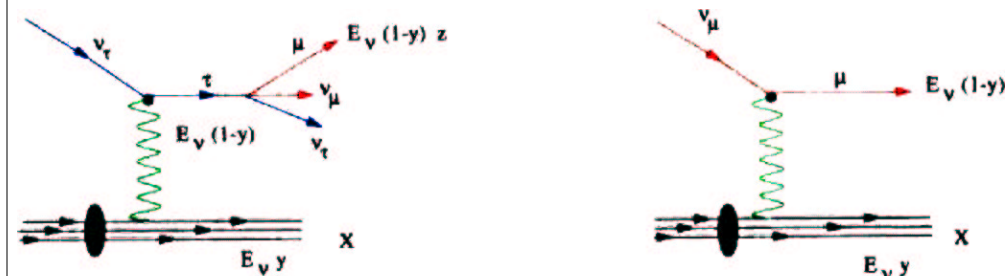
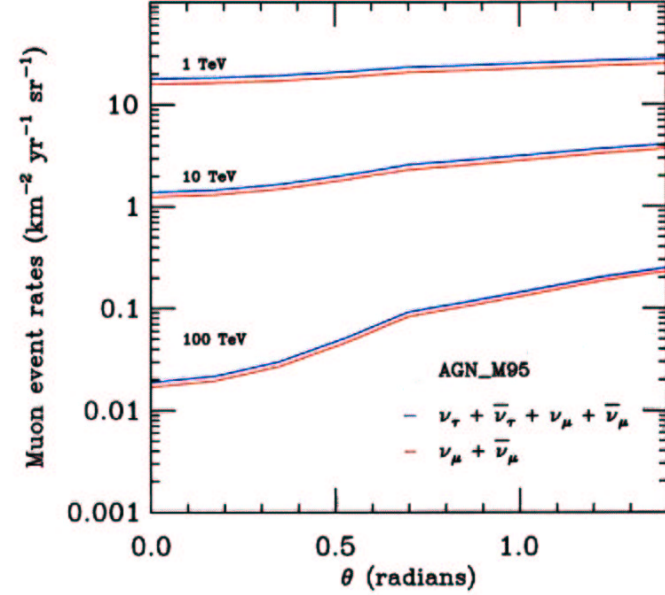
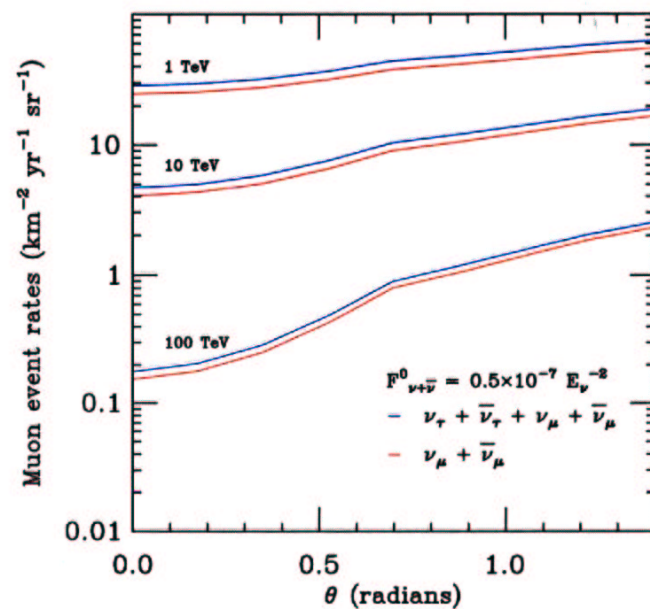
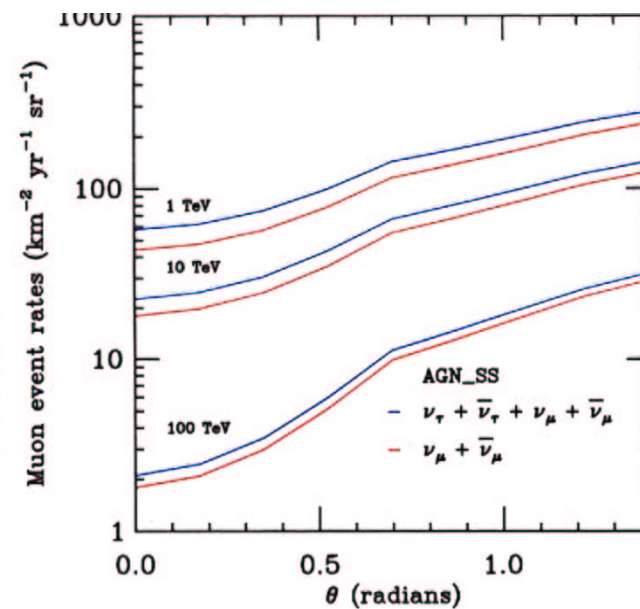
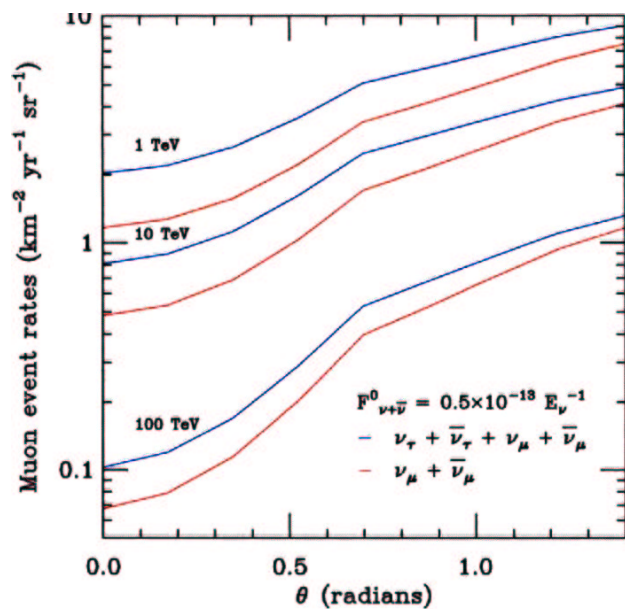
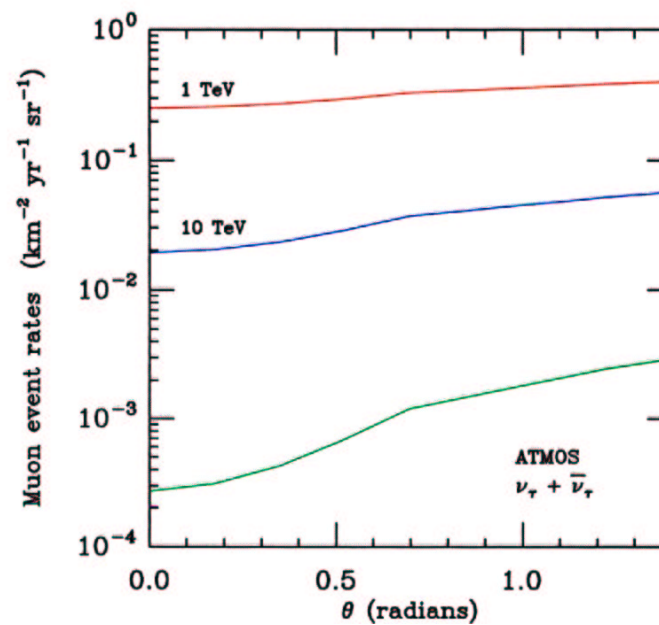
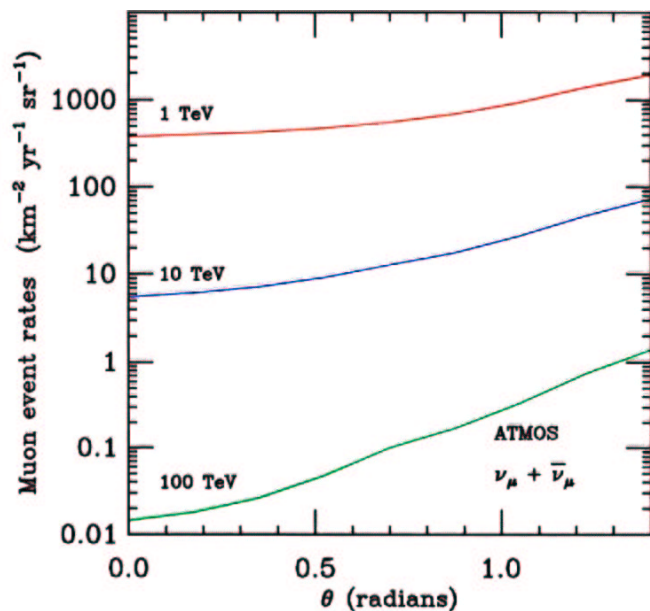


FIG. 5. Diagrams for neutrino interactions contributing to the muon production.





Is ν_τ contribution to upward muons significant?

- For steeper fluxes ν_τ contribution is about 20 – 25%

AGN M95, E^{-2}

- Enhancement is less pronounced at smaller nadir angles and for increasing threshold of energy

- For flatter fluxes the enhancement is larger, up to a factor of 2

TD SLSC, E^{-1}

- Contributions from ν and $\bar{\nu}$
- Threshold energy > 1 TeV, 10 TeV, 100 TeV
- Atmospheric background negligible at 10 TeV, 100 TeV

Background

- Shower event rates (*neutral-current contribution*):

$$R_{\nu_{\mu,e}} = V N_A \int_{E_{shr}^{min}}^{\infty} dE_{\nu} \int dy \frac{d\sigma_{nc}(E_{\nu}, y)}{dy} F_{\nu}(E_{\nu}, X) \Theta(E_{\nu}y - E_{shr}^{min})$$

- Shower event rates (*charged-current contribution*):

$$R_{\nu_e} = V N_A \int_{E_{shr}^{min}}^{\infty} dE_{\nu} \int dy \frac{d\sigma_{cc}(E_{\nu}, y)}{dy} F_{\nu}(E_{\nu}, X) \Theta(E_{\nu}y - E_{shr}^{min})$$

- Volume : 1 Km^3
- CC differential cross section : $\frac{d\sigma_{cc}(E_{\nu}, y)}{dy}$
- NC differential cross section : $\frac{d\sigma_{nc}(E_{\nu}, y)}{dy}$

Signal

- *Hadronic/Electromagnetic showers from ν_{τ} interactions:*

$$R_{\nu_{\tau}} = V N_A \int_{E_{shr}^{min}}^{\infty} dE_{\nu} \int dy \int dz \frac{dn(E_{\tau})}{dz} \frac{d\sigma_{cc}(E_{\nu}, y)}{dy}$$

$$\times F_{\nu}(E_{\nu}, X) \Theta(E_{\nu}(y + (1 - y)(1 - z)) - E_{shr}^{min})$$

- Decay distribution for τ : $\frac{dn(E_{\tau})}{dz}$
- Branching fraction for $\tau \rightarrow \nu_{\tau} \nu_{\mu} \textcolor{red}{\nu_{\tau}}$: 0.18
- $A = 1 \text{ Km}^3$

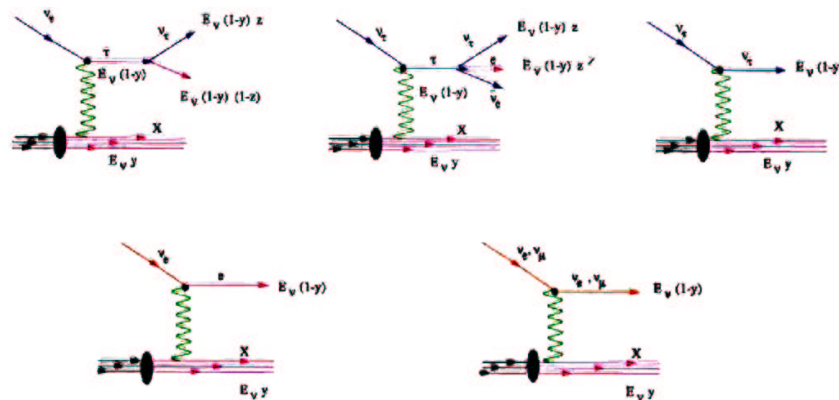
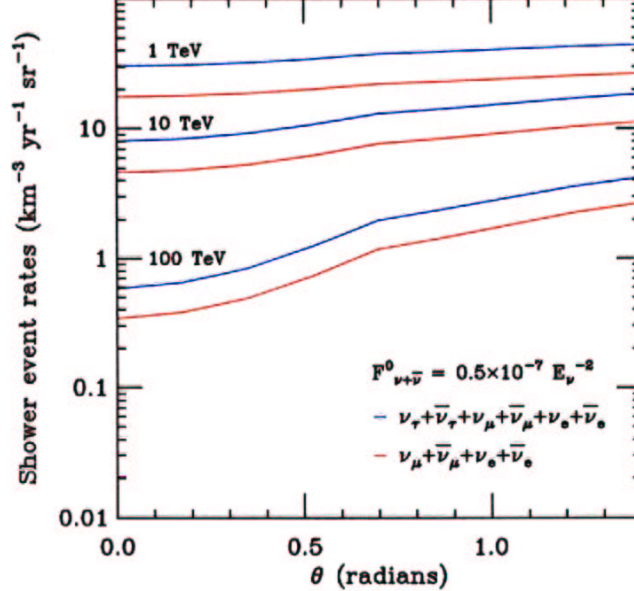
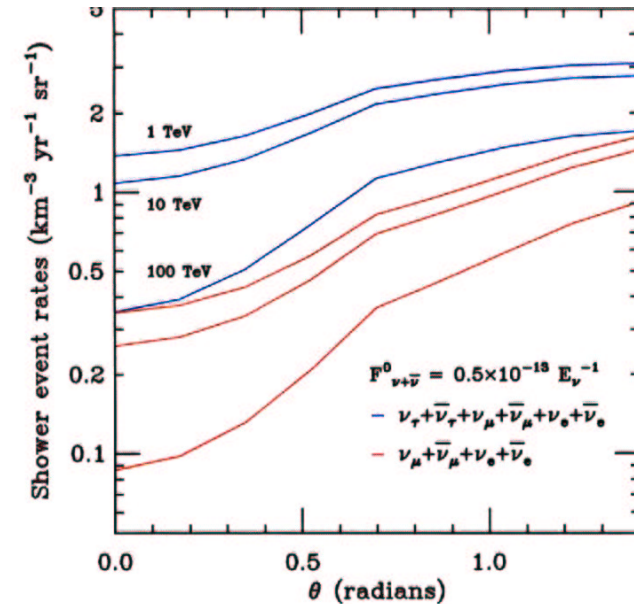
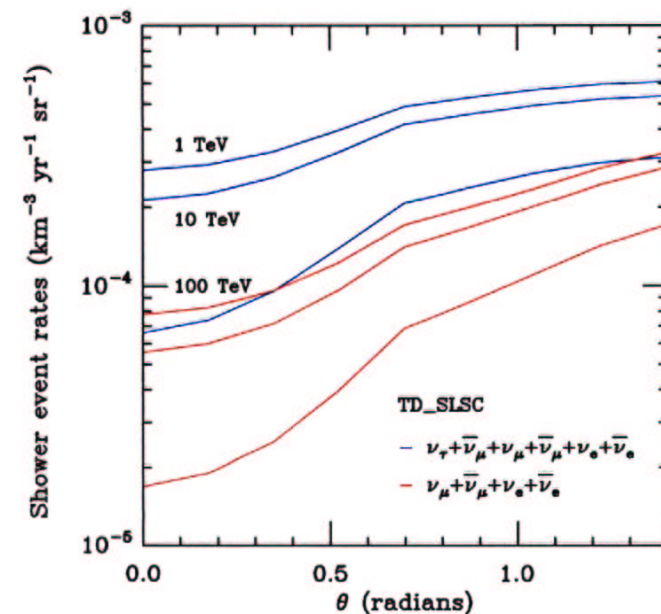
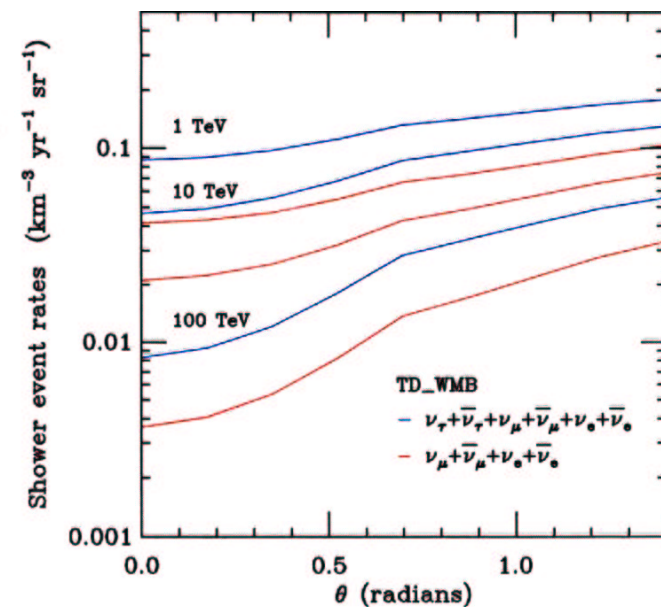
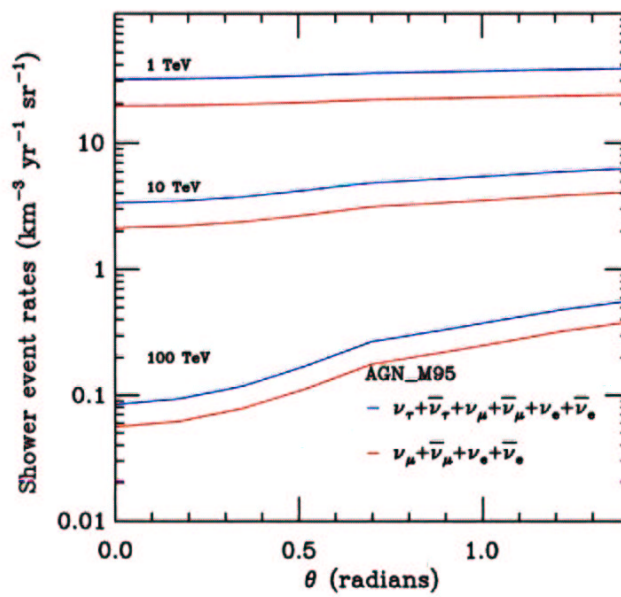
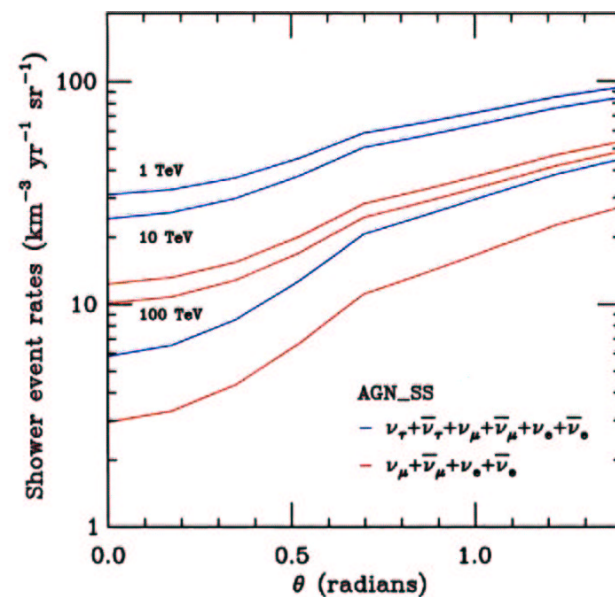
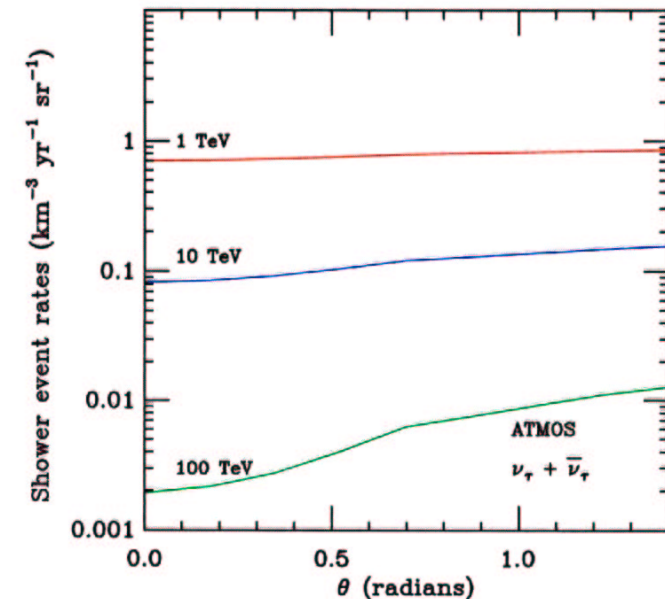
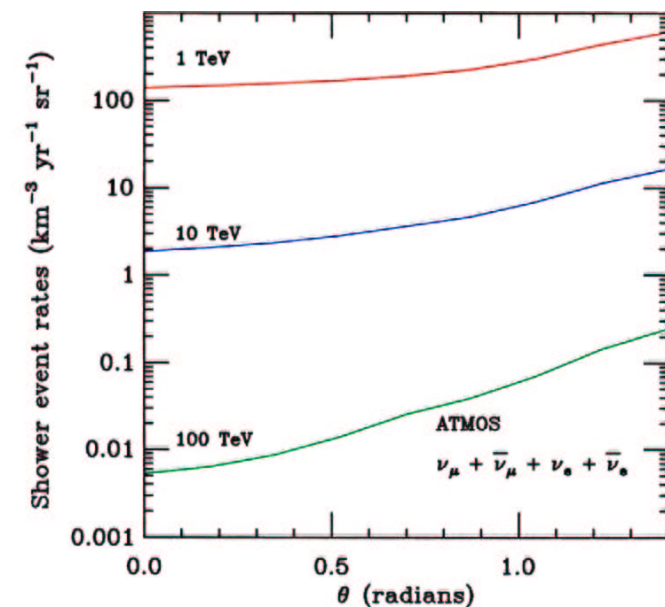
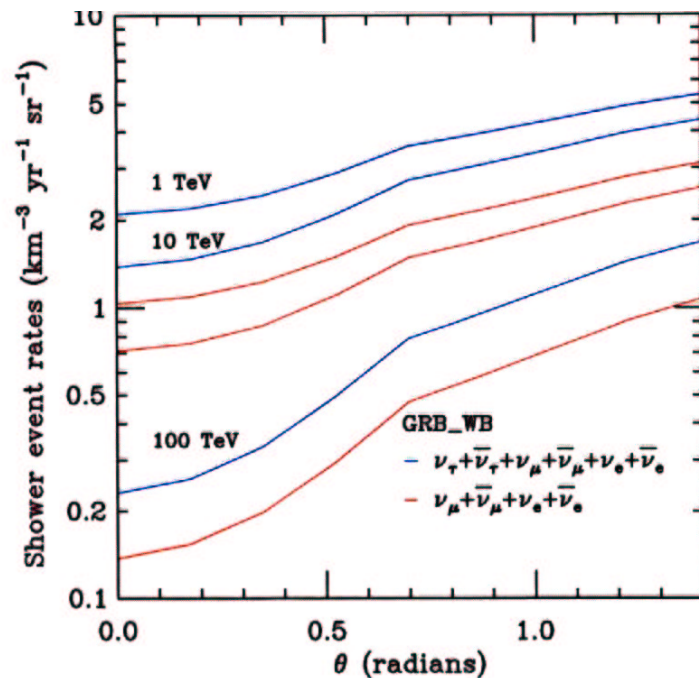


FIG. 11. Diagrams for neutrino interactions contributing to the shower events.

11





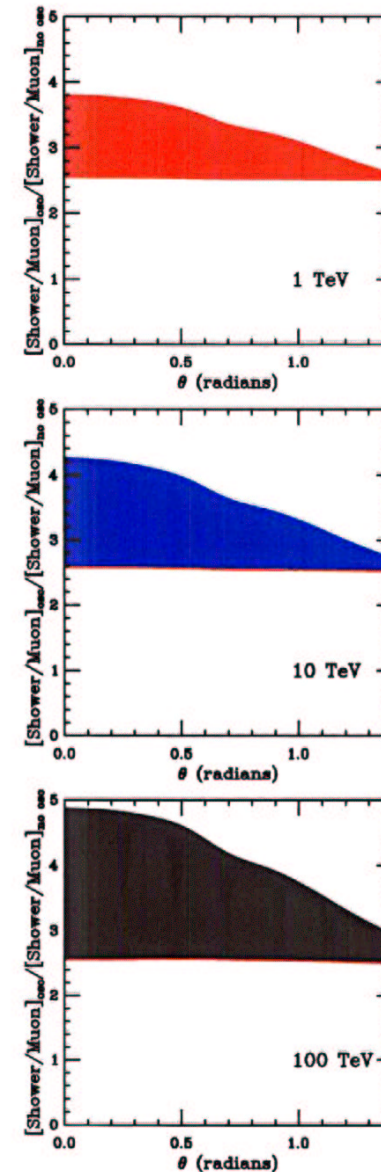


- Enhancement: factor of 4 for flatter fluxes
- Ratio of the rates for oscillation and no oscillation scenarios:

$$\text{Ratio}(R_1) = \frac{(\nu_\tau + \nu_\mu + \nu_e \rightarrow \mu)_{\text{osc}}}{(\nu_\mu + \nu_e \rightarrow \mu)_{\text{noosc}}} \sim 0.5$$

$$\text{Ratio}(R_2) = \frac{(\nu_\tau + \nu_\mu + \nu_e \rightarrow \text{shower})_{\text{osc}}}{(\nu_\mu + \nu_e \rightarrow \text{shower})_{\text{noosc}}} \sim 4.0(E^{-1}) \leftrightarrow 1.5(E^{-2})$$

- Ratio of the ratios, i.e. $(R) \equiv R_2/R_1 > 2.4$
independent of the initial flux (i.e. model independent)



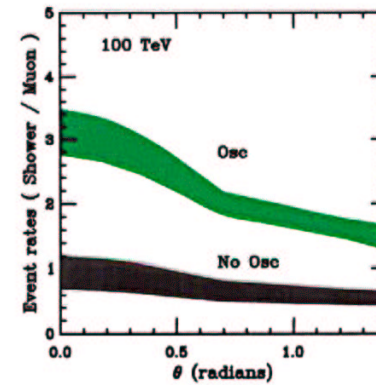
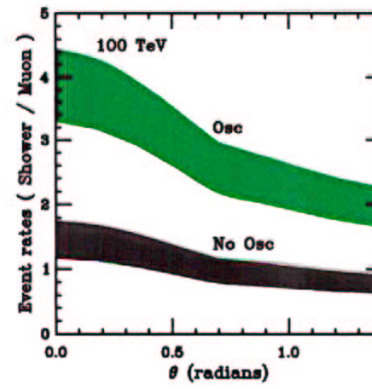
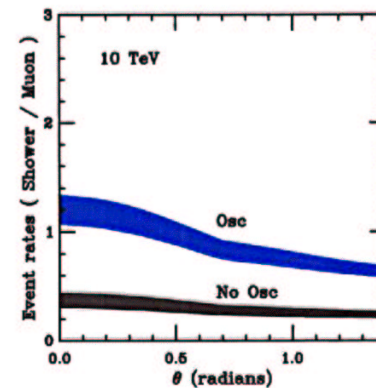
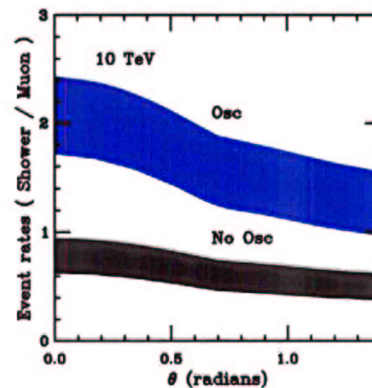
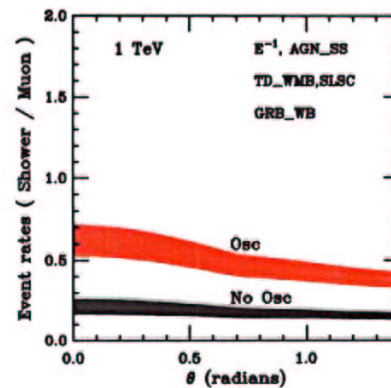
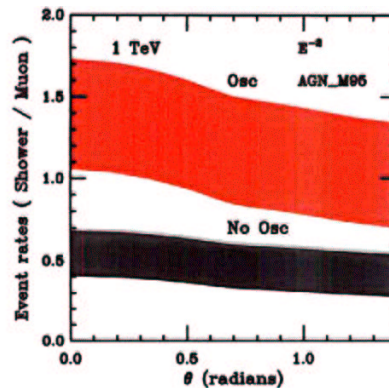


Table 1: Integrated upward shower (muon) rates per year for energy threshold of 1 TeV.

Model	E^{-1}	E^{-2}	AGN_SS	AGN_M95	GRB_WB	ATM
1+3	170(422)	2528(3255)	918(2521)	224(157)	26.9(65.8)	
2+2	141(422)	1898(3255)	726(2521)	163(157)	20.9(65.8)	
No osc	88.1(646)	1750(5676)	593(4228)	158(280)	18.3(113)	2355(7346)

Table 2: Integrated upward shower (muon) rates per year for energy threshold of 10 TeV.

Model	E^{-1}	E^{-2}	AGN_SS	AGN_M95	GRB_WB	ATM
1+3	150(217)	954(875)	809(1245)	34.4(20.2)	21.3(28.4)	
2+2	124(217)	706(875)	633(1245)	24.5(20.2)	16.3(28.4)	
No osc	75.4(342)	652(1540)	514(2139)	24.4(36.3)	14.2(49.7)	58.45(175.5)

Table 3: Integrated upward shower (muon) rates per year for energy threshold of 100 TeV.

Model	E^{-1}	E^{-2}	AGN_SS	AGN_M95	GRB_WB	ATM
1+3	84.8(54.2)	182(100)	386(255)	2.46(0.999)	7.28(4.03)	
2+2	68.4(54.2)	130(100)	285(255)	1.69(0.999)	5.21(4.03)	
No osc	42.0(91.3)	124(182)	251(460)	1.78(1.83)	4.99(7.31)	0.7735(1.39)

- For energies above 10^6 GeV, of relevance to OWL/EUSO, we need to include the energy loss of the τ propagating through the Earth.

- Energy loss processes for muons and taus:

- * Bremsstrahlung
- * Ionization
- * Pair Production
- * Photonuclear Processes

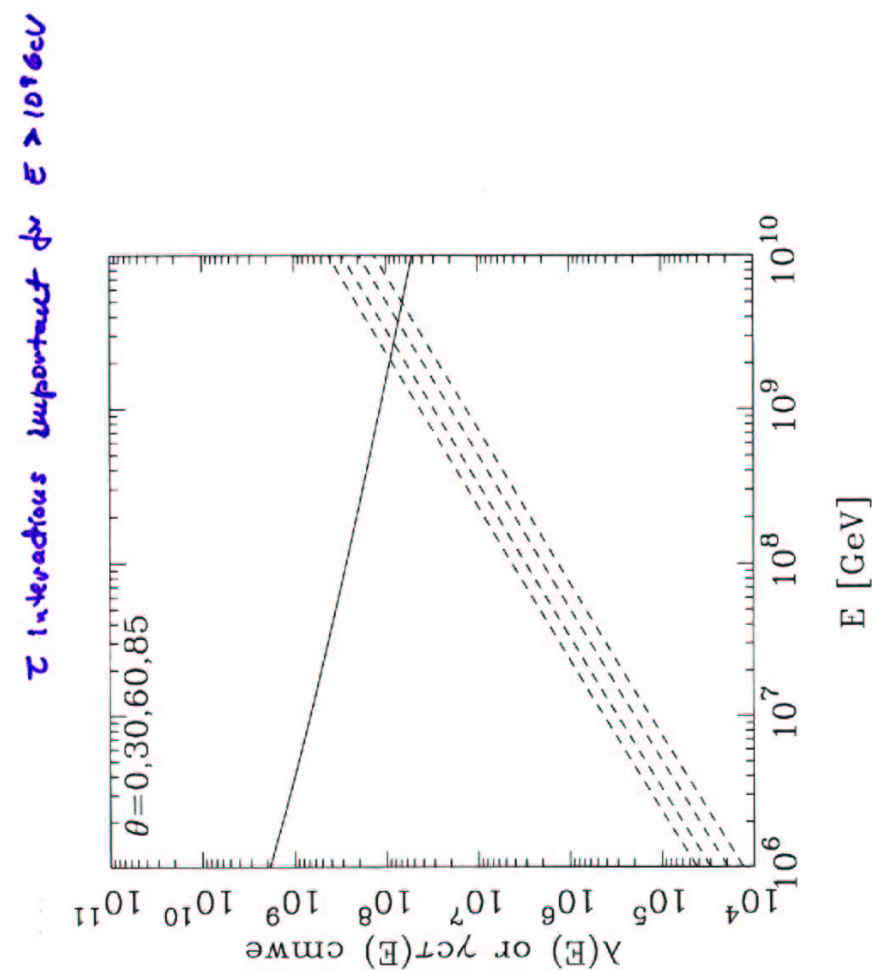
S.I. Dutta, M.H. Reno, I. Sarcevic and D. Seckel,
PRD63, 094020 (2001).

- For energies above 10^6 GeV, new physics might become relevant, such as exchange of bulk gravitons (i.e. Kaluza-Klein modes) in the neutral-current interactions.

(Fig)

- Possibility of testing theory of large extra dimensions with ultrahigh energy neutrinos?

P. Jain, D.W. Mc Kay, S. Panda and J. Ralston, PLB484, 267 (2000).
 C. Tyler, A. Olinto and G. Sigl, PRD63, 055001 (2001).
 S. Nussinov and R. Shrock, PRD59, 105002 (1999); hep-ph/0103043.
 H. Davoudiasl, J.L. Hewett and T.G. Rizzo, hep-ph/0010066.



Ultrahigh Energy Neutrinos as Probes of New Physics

Even before the LHC, new TeV-scale physics may be observed in the scattering of ultrahigh energy ($E_\nu > 100 \text{ TeV}$) cosmic or extragalactic neutrinos off nuclei in air or ice and detected by neutrino telescopes such as AMANDA, ICECUBE or RICE or with cosmic ray air shower detectors such as Pierre Auger or AGASA or with the satellite experiments, such as EUSO and OWL.

- Possibility that we live in $4 + n$ spacetime dimensions has profound implications. If gravity propagates in these extra dimensions, the fundamental Planck scale, M_D , at which gravity becomes comparable in strength to other forces, may be far below $M_{Pl} \sim 10^{19} \text{ GeV}$, in TeV range, leading to a host of potential signatures for high energy physics \Rightarrow one of the most striking consequences of low-scale gravity is the possibility of black hole creation in high-energy particle collisions.
- Most gravitation processes, such as those involving graviton emission and exchange, analyses rely on a perturbative description that breaks down for energies of M_D and above.
- In contrast, black hole properties are best understood for energies above M_D , where semiclassical and thermodynamic descriptions become increasingly valid.

- Particle scattering at super-Planckian energies is dominated in the s-channel by black hole production. Thus, black holes provide a robust probe of extra dimensions and low-scale gravity, as long as particle collisions with energies above M_D are available.
- Copious production of microscopic black holes is one of the least model-dependent predictions of TeV-scale gravity scenarios.
- Ultrahigh energy neutrinos ($E_\nu > 100$ TeV) can provide unique probe of the large extra spacetime dimensions \Rightarrow detection of the black hole formation in neutrino interactions would reveal the structure of the extra dimensions on scales large as compared to the Planck scale.

Collider Limits:

• Fermilab:

$$M_\star > 530 \text{ GeV for } n = 4$$

$$M_\star > 580 \text{ GeV for } n = 6$$

$$M_\star > 680 \text{ GeV for } n = 8$$

• LEPII:

$$M_\star > 680 \text{ GeV for } n = 4$$

$$M_\star > 510 \text{ GeV for } n = 6$$

$$M_\star > 411 \text{ GeV for } n = 8$$

Astrophysical and Cosmological Constraints:

- Supernova cooling
- Neutron Star heat excess
- Cosmology (Cosmic Microwave Background Radiation and Cosmic Gamma-Ray Background Radiation – cooling rate)

$M_\star > 600 \text{ TeV}$ for $n = 2$

$M_\star > 30 \text{ TeV}$ for $n = 3$

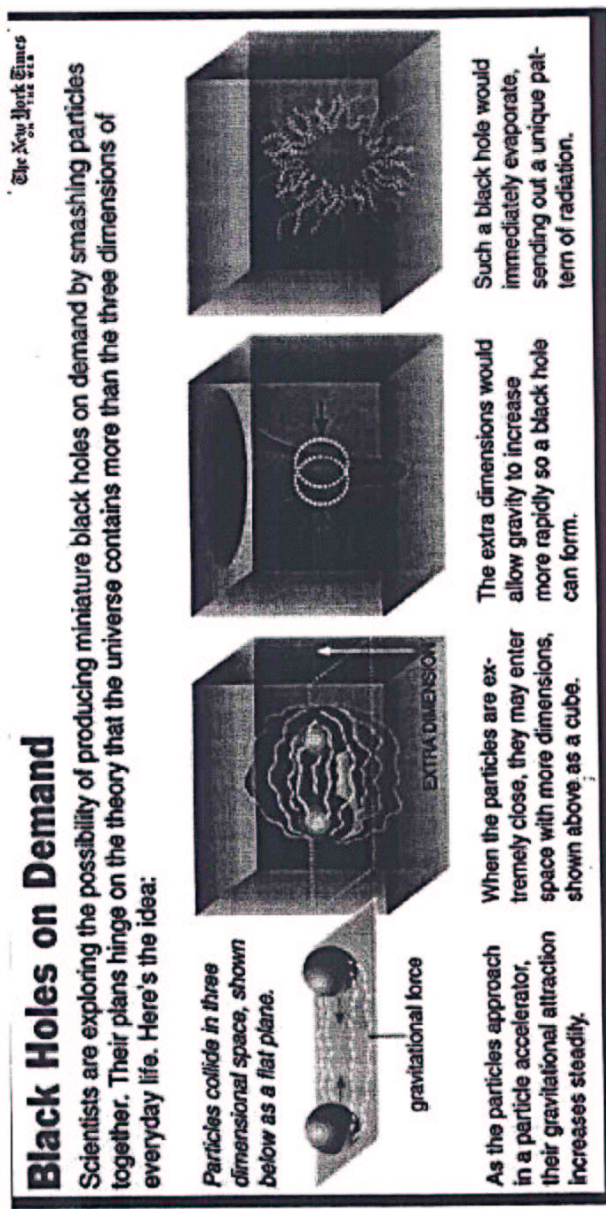
Astrophysical and Cosmological Constraints imply that $n = 2$ and $n = 3$ are ruled out!

Black Holes in General Relativity

- Schwarzschild solution to Einstein's general relativity equations applied to a static massive object has a singularity at a Schwarzschild radius. If the radius of the object is less than R_S , a black hole with the event horizon at R_S is formed.
- According to Hawking, black holes are unstable semi-classically and evaporate, i.e. decay into thermal spectrum of particles.
- As the BH evaporates, its mass becomes smaller and the Hawking temperature increases.

Black Holes in Higher Dimensional Space-Time

- Static BH solution in $N+1$ dimensions is a generalization of familiar Schwarzschild solution
Myers and Perry, Annals of Phys. 172, 304 (1986).
- BH radiates mainly on the brane
Emparan, Horowitz and Myers, PRL 85, 499 (2000).



Assumptions:

- To avoid stringy effects and be able to use semi-classical approach we consider $M_{BH} \gg M_D$
- Decay: BH evaporation at the original temperature
- BH radiates mainly on the brane
- Most of the decay is hadronic
- Typical lifetime 10^{-27} s.
- Lack of knowledge of quantum gravity effect close to the Planck scale – theoretical input needed
- Greybody factors recently calculated in $\omega r_S \ll 1$ approximation

- The cross-section for black hole production in pp collisions, for example, is obtained by folding in the parton densities:

$$\sigma(pp \rightarrow BH + X) = \frac{1}{s} \sum_{ab} \int_{M_{BH,min}^2}^s dM_{BH}^2$$

$$\times \int_{x_{1,min}}^1 \frac{dx_1}{x_1} f_a(x_1, Q^2) \hat{\sigma}_{BH} f_b(x_2, Q^2)$$

- Radiation rate into Standard Model particles is given by a thermal distribution in 4 dimensions:

$$\frac{dE}{dt} = \frac{1}{(2\pi)^3} \sum_i \int \frac{\omega g_i \sigma_i d^3 k}{e^{\omega/T_{BH}} \pm 1}$$

with $T_{BH} = \frac{d-3}{4\pi r_S}$, g_i ia a statistical factor, accounting for the number of degrees of freedom that can be produced. The sign $+$ is for fermions and $-$ for bosons, σ_i are the gray body factors, $\sigma_i \approx \Gamma_s A_4$, where Γ_s are constant ($\Gamma_{1/2} = 2/3, \Gamma_1 = 1/4, \Gamma_0 = 1$).

- A black hole acts as an absorber with a radius somewhat larger than r_S , such that A_n is given by

$$A_n = \Omega_{n-2} \left(\frac{d-1}{2}\right)^{\frac{d-2}{d-3}} \left(\frac{d-1}{d-3}\right)^{\frac{n-2}{2}} r_S^{n-2}$$

Emparan, Horowitz, Myers, PRL 85, 499 (2000).

- For the emission into gravitons, which are d-dimensional, the rate is given by:

$$\frac{dE}{dt} = \frac{1}{(2\pi)^{d-1}} \sum_i \int \frac{\omega g_i \sigma_i d^{d-1} k}{e^{\omega/T_{BH}} - 1}$$

where $\sigma_i \sim A_{d-1}$. This rate is much smaller than emission rate into SM particles.

- The lifetime of the black hole is then obtained by integrating rate equation and, assuming no mass evolution during the decay, is given by:

$$\tau_{BH} = M_{BH} \left[\frac{\pi^2}{30} \left(\sum_f \frac{7}{8} g_f \sigma_f + \sum_b g_b \sigma_b \right) T_{BH}^4 \right]^{-1}$$

- The energy radiated in n dimensions by a d -dimensional black hole with temperature T is

$$\frac{dE_n}{dt} \simeq \int \frac{\omega^{n-1} d\omega A_n}{e^{\omega/T} - 1}$$

where A_n is the area of the black hole in n dimensions,

$$A_n = \Omega_n r_S^n \quad T = \frac{d-3}{4\pi r_S} \quad \Omega_{n-1} = \frac{2\pi^{n/2}}{\Gamma(n/2)}$$

Ω_n is the volume of a unit n sphere

$$\frac{dE_n}{dt} \simeq \frac{1}{(2\pi)^{n-1}} \Gamma(n) \zeta(n) \Omega_{n-2}^2 \left(\frac{d-3}{4\pi}\right)^n \frac{1}{r_S^2}$$

- The black hole is a d -dimensional object and it radiates in all dimensions with a rate dE_n/dt . However, Standard Model fields are four dimensional fields that live on the brane, thus the rate of emission on the brane is dE_4/dt .
- The ratio of emission rates in 4 dimensions and in n dimensions is:

$$\frac{dE_4/dt}{dE_n/dt} \sim 10$$

thus most of the radiation is on the brane, in SM particles.

Black Hole Production by UHE Neutrinos

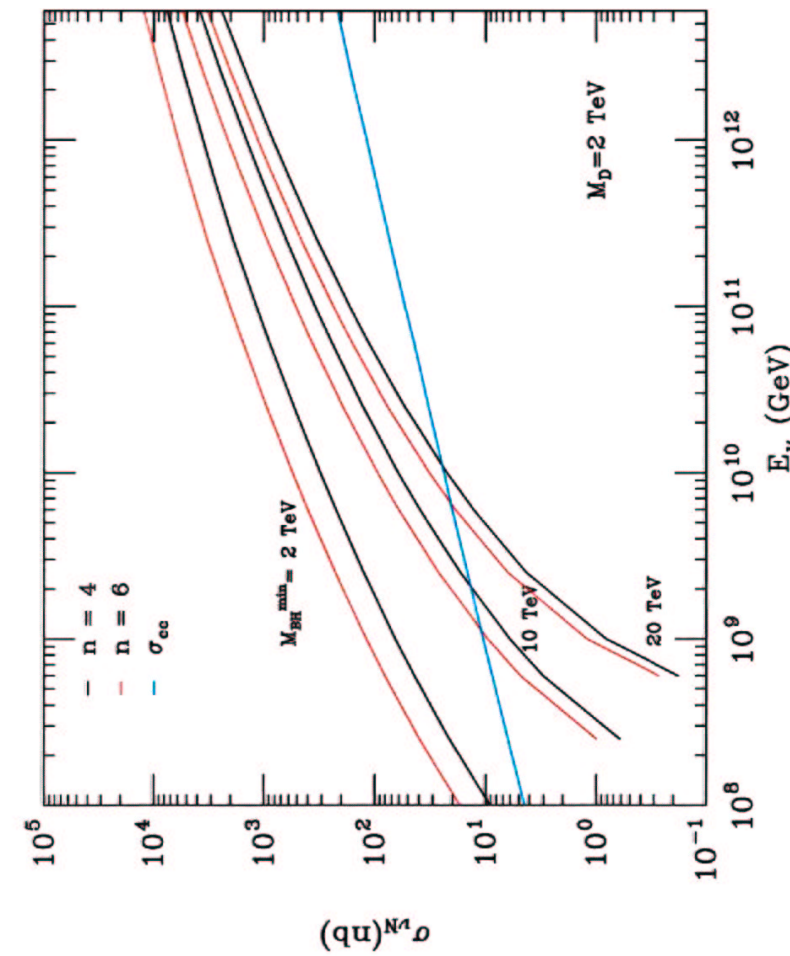
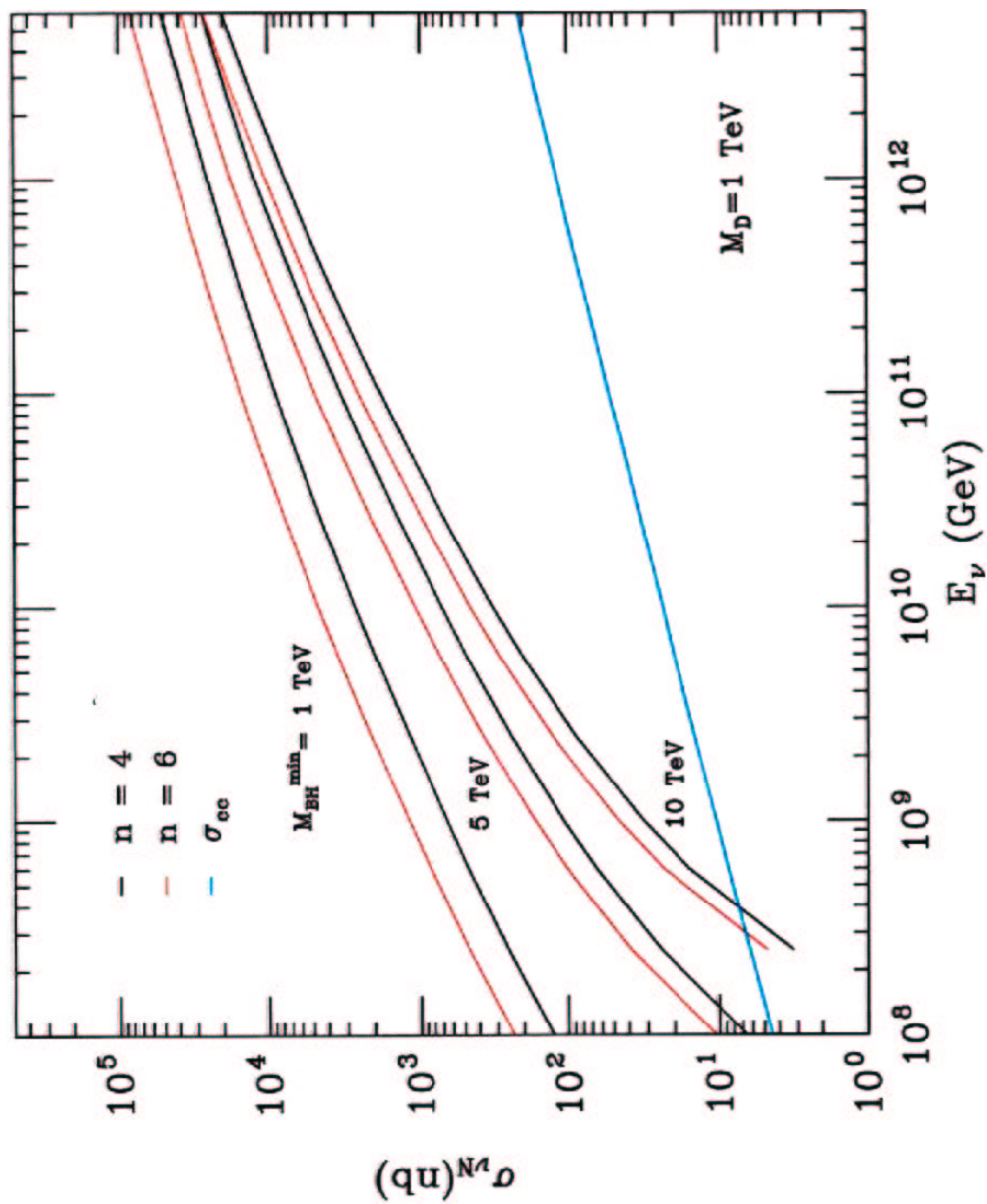
- Black hole can be produced in scattering of UHE neutrinos on nucleons in the atmosphere or in the Earth. The neutrino-nucleon cross section for black hole production is given by

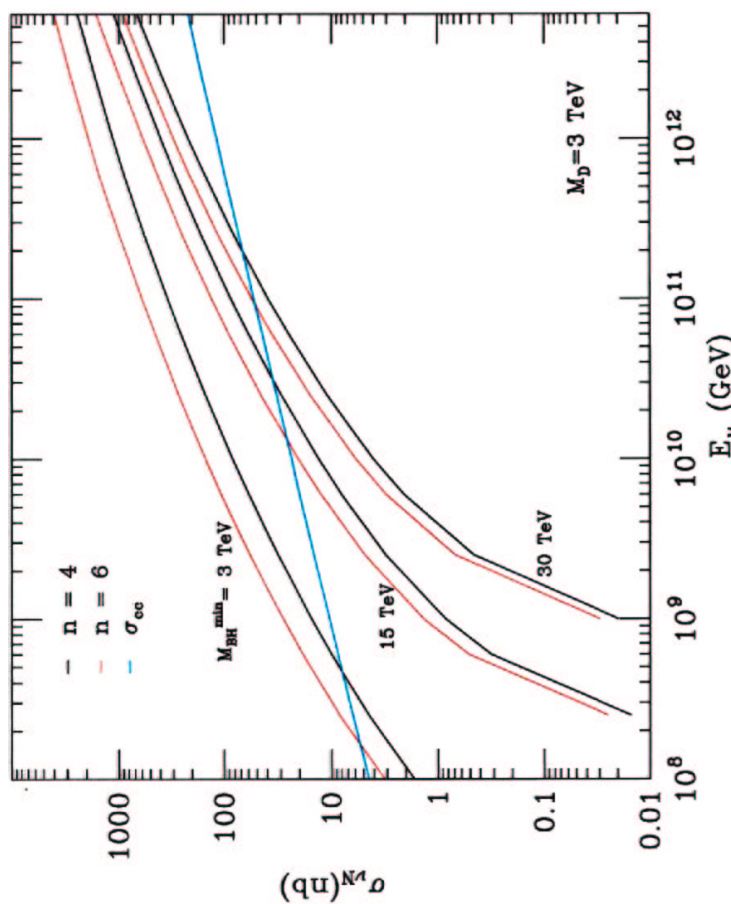
$$\sigma(\nu N \rightarrow \text{BH}) = \sum_i \int_{M_{BH}^{\min}}^1 dx \hat{\sigma}_i(xs) f_i(x, Q^2),$$

where

$$\hat{\sigma}_i = \pi r_S^2 (M_{BH} = \sqrt{\hat{s}}) \theta(\sqrt{\hat{s}} - M_{BH}^{\min}),$$

$\hat{s} = xs$, s is the center of mass energy, $s = 2m_N E_\nu$
 $f_i(x, Q^2)$'s are parton distribution functions
 M_{BH}^{\min} is the minimum black hole mass for which semiclassical approximation above is valid ($M_{BH}^{\min} >> M_D$)





Black Holes in Cosmic Rays

Feng and Shapere, PRL 88 (2002) 021303.
Anchordoqui, Feng, Goldberg and Shapere,
PR D65 (2002) 124027.

- Limits from non-observation of horizontal showers by the Fly's Eye Collaboration and Akeno Giant Air Shower Array (AGASSA): $M_D \approx 1 \text{ TeV} - 1.4 \text{ TeV}$ excluded for $n \geq 4$.
- Detect BH in the Pierre Auger fluorescence experiment or AGASSA \Rightarrow few to a hundred BHs can be detected before the LHC turns on. If no black holes are found then $M_D = 2 \text{ TeV}$ is excluded for any n .

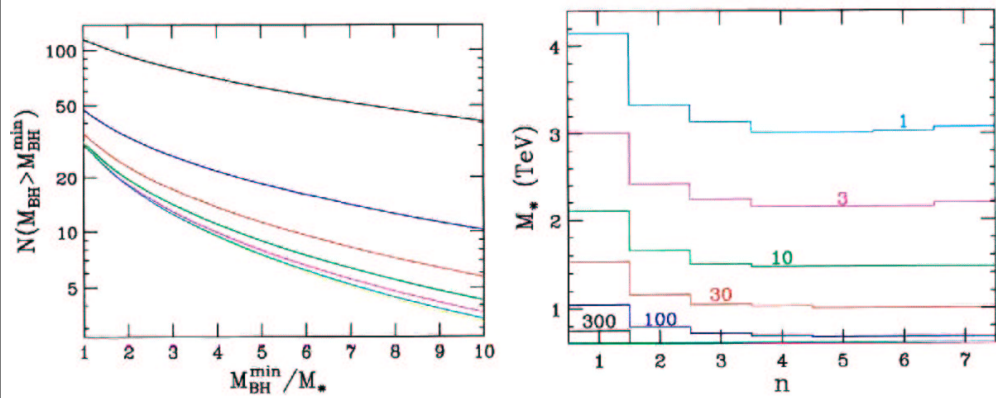


Figure 1: The number of BH events detected in 5 Auger site-years a) $M_* = 1 \text{ TeV}$; b) $M_* = M_{\text{BH}}^{\text{min}}$

Black Holes in Neutrino Telescopes

Alvarez-Muniz, Feng, Halzen, Tan and Hooper,
 PRD **65**, 124015 (2002)
 Kowalski, Ringwald and Tu, PL B529, 1 (2002)
 Dutta, Reno and Sarcevic, PR D66, 033002 (2002)

- The contained event rate for black hole production is

$$\text{Rate} = \int dE_\nu N_A V_{eff} \sigma_{BH}(E_\nu) \frac{dN_\nu}{dE_\nu}$$

N_A is Avogadro's number

$\frac{dN_{\nu\mu}}{dE_{\nu\mu}}$ is the neutrino flux that reaches the detector
 V_{eff} is the effective volume of the detector.

Event Rates for ICECUBE

Contained event rates per year for $M_D = 1$ TeV ($m = M_{BH}^{\min}/M_D$) and $E_{sh}^{\min} = 10^8$ GeV.

n = 4

m	E^{-1}	E^{-2}	GRB_{WB}	TD_{WMB}	TD_{SLSC}	AGN_{M95}	AGN_{SS}	COS_{STD}	COS_{STR}
1	5447.0	444.3	0.481	56.01	0.563	32.73	9.348	2.16	5.89
2	2430.0	225.0	0.206	34.30	0.285	15.96	3.767	1.19	3.16
3	1363.0	141.1	0.112	24.77	0.177	9.65	1.923	0.79	2.06
4	848.2	97.9	0.067	19.26	0.121	6.45	1.082	0.57	1.47
5	560.0	72.0	0.043	15.65	0.088	4.57	0.636	0.43	1.11

n = 6

1	9930.0	797.9	0.879	97.46	1.013	59.14	17.190	3.85	10.50
2	4161.0	378.8	0.355	55.99	0.481	27.07	6.514	1.98	5.29
3	2250.0	228.5	0.186	38.92	0.288	15.76	3.210	1.26	3.32
4	1364.0	154.0	0.109	29.45	0.192	10.25	1.762	0.89	2.31
5	881.7	110.9	0.068	23.42	0.137	7.12	1.016	0.66	1.71

SM	136	8.4	0.01	0.65	0.01	0.6	0.3	0.03	0.09
----	-----	-----	------	------	------	-----	-----	------	------

Contained event rates per year for $M_P = 2\text{TeV}$ and $E_{\gamma h}^{\min} = 10^8 \text{ GeV}$

4

m	E^{-1}	E^{-2}	GRB_{WB}	TD_{WMB}	TD_{SISc}	AGN_{M95}	AGN_{ss}	COS_{STD}	COS_{STR}
$n = 6$									
2	460.3	42.63	0.39E-01	6.50	0.54E-01	3.023	0.71E+00	0.225	0.599
4	160.7	18.54	0.13E-01	3.65	0.23E-01	1.222	0.21E+00	0.108	0.279
6	72.7	10.47	0.54E-02	2.48	0.13E-01	0.639	0.72E-01	0.065	0.165
8	36.2	6.68	0.24E-02	1.85	0.77E-02	0.375	0.23E-01	0.044	0.109
10	19.9	4.65	0.12E-02	1.45	0.51E-02	0.238	0.91E-02	0.031	0.077
SM	136	8.4	0.01	0.65	0.01	0.6	0.3	0.03	0.09

Contained event rates per year for $M_D = 3\text{TeV}$ and $E_{\text{shr}}^{\min} = 10^8 \text{ GeV}$.

n = 4

<i>m</i>	E^{-1}	E^{-2}	GRB_{WB}	TD_{WMB}	TD_{SLSC}	AGN_{M95}	AGN_{SS}	COS_{STD}	COS_{STR}
3	97.6	10.11	0.80E-02	1.77	0.13E-01	0.691	0.14E+00	0.56E-01	0.15E+00
6	27.5	3.96	0.20E-02	0.94	0.48E-02	0.241	0.27E-01	0.25E-01	0.62E-01
9	9.9	2.08	0.61E-03	0.62	0.24E-02	0.112	0.47E-02	0.14E-01	0.34E-01
12	4.4	1.30	0.23E-03	0.45	0.13E-02	0.061	0.66E-03	0.88E-02	0.22E-01
15	2.0	0.88	0.98E-04	0.34	0.81E-03	0.035	0.11E-03	0.60E-02	0.14E-01

n = 6

3	182.6	18.55	0.15E-01	3.16	0.23E-01	1.280	0.26E+00	0.10E+00	0.27E+00
6	48.2	6.77	0.36E-02	1.56	0.82E-02	0.419	0.49E-01	0.42E-01	0.11E+00
9	16.6	3.42	0.10E-02	0.98	0.39E-02	0.187	0.80E-02	0.23E-01	0.56E-01
12	7.1	2.06	0.38E-03	0.70	0.22E-02	0.099	0.11E-02	0.14E-01	0.34E-01
15	3.2	1.36	0.16E-03	0.52	0.13E-02	0.056	0.17E-03	0.94E-02	0.22E-01

SM 136 8.4 0.01 0.65 0.01 0.6 0.3 0.03 0.09

Alvarez-Huerta, Feng, Halzen, Hauke
 arXiv:hep-ph/0202081

TABLE I: Event rate for down-going showers (in 2π sr) with $E_{\text{sh}}^{\text{thr}} = 500$ TeV in IceCube. We consider the Waxman-Bahcall [51] and cosmogenic [46] fluxes, $M_D = 1$ and 2 TeV, and various cases ($n, x_{\min}, \bar{\sigma}$), where n is the number of extra dimensions, $x_{\min} \equiv M_{\text{BH}}^{\text{min}}/M_D$, and $\bar{\sigma}$ is the parton level cross section for black hole production.

Showers ($\text{km}^{-3} \text{ yr}^{-1}$)	WB Flux		Cosmogenic Flux	
	$M_D = 1 \text{ TeV}$	$M_D = 2 \text{ TeV}$	$M_D = 1 \text{ TeV}$	$M_D = 2 \text{ TeV}$
Standard Model	4.8	4.8	0.1	0.1
BH (6, 1, πr_s^2)	44.6	3.1	5.2	0.9
BH (6, 3, πr_s^2)	6.5	0.5	2.3	0.3
BH (6, 1, $\pi r_s^2 e^{-I}$)	18.5	1.2	2.1	0.3
BH (6, 3, $\pi r_s^2 e^{-I}$)	0.4	2.8×10^{-2}	0.1	1.5×10^{-2}
BH (3, 1, πr_s^2)	16.3	1.1	2.7	0.4
BH (3, 3, πr_s^2)	3.0	0.2	1.2	0.1
BH (3, 1, $\pi r_s^2 e^{-I}$)	3.8	0.2	0.5	6.1×10^{-2}
BH (3, 3, $\pi r_s^2 e^{-I}$)	2.9×10^{-2}	1.9×10^{-3}	8.6×10^{-3}	9.3×10^{-4}

TABLE II: As in Table I, but for the flux of down-going muons and $E_{\mu}^{\text{thr}} = 500$ TeV.

Muons ($\text{km}^{-2} \text{ yr}^{-1}$)	WB Flux		Cosmogenic Flux	
	$M_D = 1 \text{ TeV}$	$M_D = 2 \text{ TeV}$	$M_D = 1 \text{ TeV}$	$M_D = 2 \text{ TeV}$
Standard Model	6.0	6.0	0.2	0.2
BH (6, 1, πr_s^2)	27.7	2.6	4.9	1.1
BH (6, 3, πr_s^2)	12.0	1.1	4.9	0.7
BH (6, 1, $\pi r_s^2 e^{-I}$)	8.8	0.7	1.3	0.2
BH (6, 3, $\pi r_s^2 e^{-I}$)	0.6	4.6×10^{-2}	0.2	2.5×10^{-2}
BH (3, 1, πr_s^2)	14.0	1.2	4.2	0.6
BH (3, 3, πr_s^2)	7.1	0.6	3.5	0.4
BH (3, 1, $\pi r_s^2 e^{-I}$)	1.8	0.1	0.3	4.1×10^{-2}
BH (3, 3, $\pi r_s^2 e^{-I}$)	4.2×10^{-2}	3.1×10^{-3}	1.5×10^{-2}	1.6×10^{-3}

TABLE III: As in Table I, but for the flux of down-going taus and $E_{\tau}^{\text{thr}} = 2.5 \times 10^6$ GeV.

Taus ($\text{km}^{-2} \text{ yr}^{-1}$)	WB Flux		Cosmogenic Flux	
	$M_D = 1 \text{ TeV}$	$M_D = 2 \text{ TeV}$	$M_D = 1 \text{ TeV}$	$M_D = 2 \text{ TeV}$
Standard Model	0.9	0.9	0.1	0.1
BH (6, 1, πr_s^2)	15.1	2.2	5.0	1.2
BH (6, 3, πr_s^2)	7.7	1.0	4.5	0.7
BH (6, 1, $\pi r_s^2 e^{-I}$)	4.5	0.6	1.3	0.2
BH (6, 3, $\pi r_s^2 e^{-I}$)	0.5	4.4×10^{-2}	0.2	2.9×10^{-2}
BH (3, 1, πr_s^2)	8.7	1.1	4.1	0.7
BH (3, 3, πr_s^2)	4.8	0.6	3.1	0.4
BH (3, 1, $\pi r_s^2 e^{-I}$)	1.0	0.1	0.4	5.2×10^{-2}
BH (3, 3, $\pi r_s^2 e^{-I}$)	2.9×10^{-2}	2.8×10^{-3}	1.6×10^{-2}	1.8×10^{-3}

Detection of Black Holes with OWL

Dutta, Reno and Sarcevic, PR D66, 033002 (2002)

The event rate for black hole production with OWL is given by

$$N = \int A(E_\nu) \frac{dN}{dE_\nu} \sigma_{BH}(E_\nu) dE_\nu$$

where

$A(E_\nu)$ is the OWL effective aperture

$\frac{dN}{dE_\nu}$ is the neutrino flux

$\sigma_{BH}(E_\nu)$ is the cross section for the production of black hole.

Tau Events in km^3 Detector from BH Production

Alvarez-Muniz et al., PR D65 (2002) 124015.

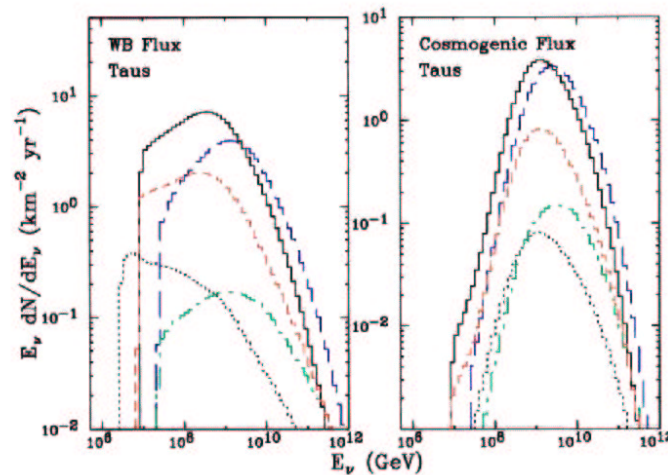


Figure 2: Energy distribution of down-going taus with $E_\tau^{thr} = 2.5 \times 10^6 \text{ GeV}$

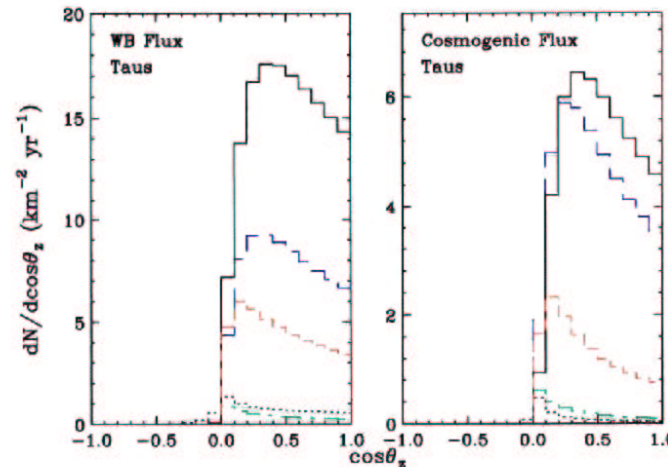


Figure 3: Zenit angle distribution of down-going taus with $E_\tau^{thr} = 2.5 \times 10^6 \text{ GeV}$

NEUTRINOS WITH OWL / Airwatch

4

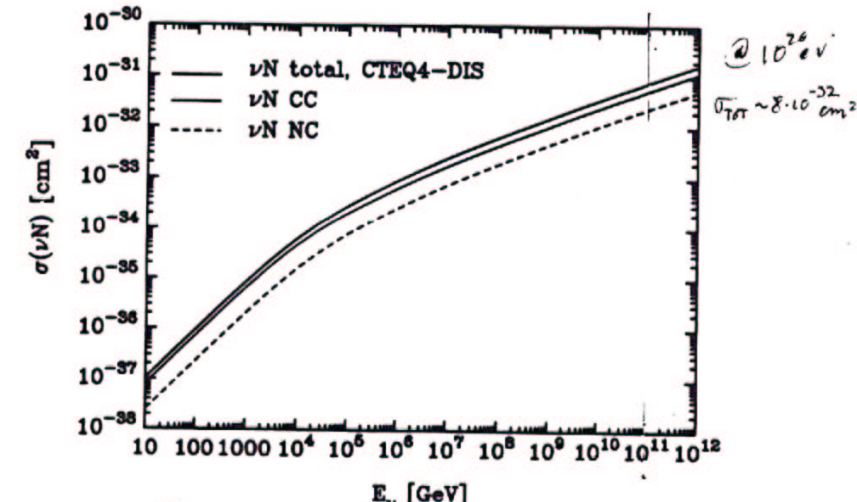
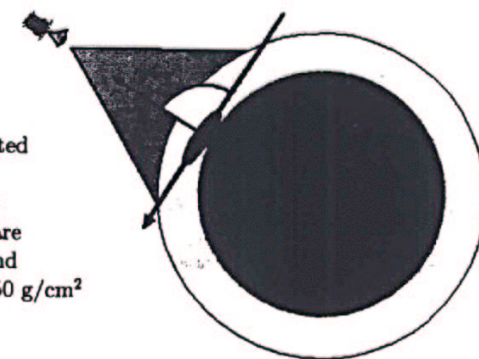
Large Aperture (10^{13} mtons of atmospheric target) opens the door for observing ultra-high energy neutrinos interactions

Value of $\sigma_{CC}(\nu_\lambda N \rightarrow \lambda N')$

$$\longrightarrow \lambda_\nu \sim 10^{10} \text{ cm}$$

(Air, STP, $E_\nu = 10^{20} \text{ eV}$)

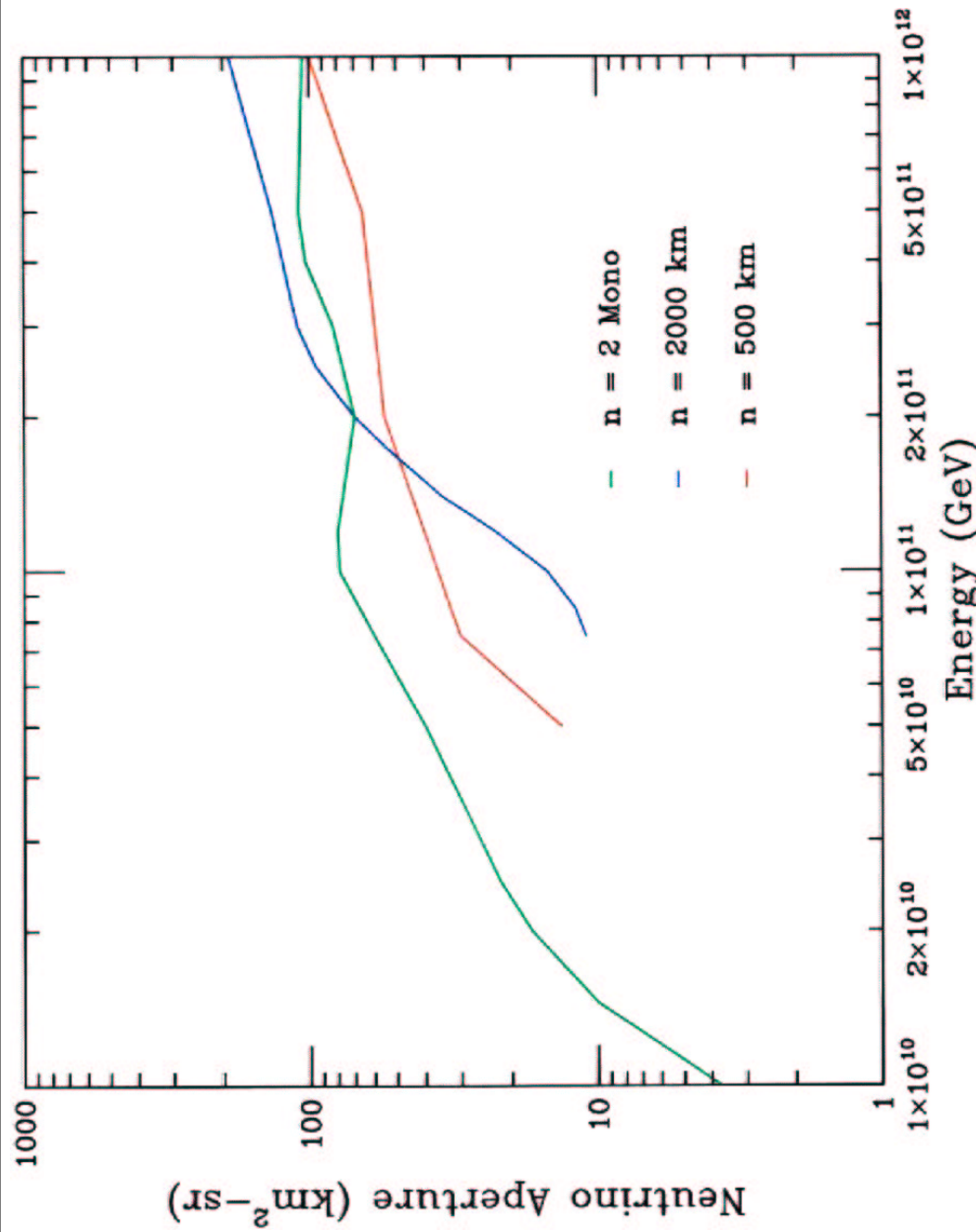
→ Horizontal Airshowers initiated deep ($> 1500 \text{ g/cm}^2$) in the atmosphere provide a signature of neutrino interactions which are well-separated from hadronic and electromagnetic showers, $\lambda_p \sim 50 \text{ g/cm}^2$
(Air, STP, $E_p = 10^{20} \text{ eV}$)

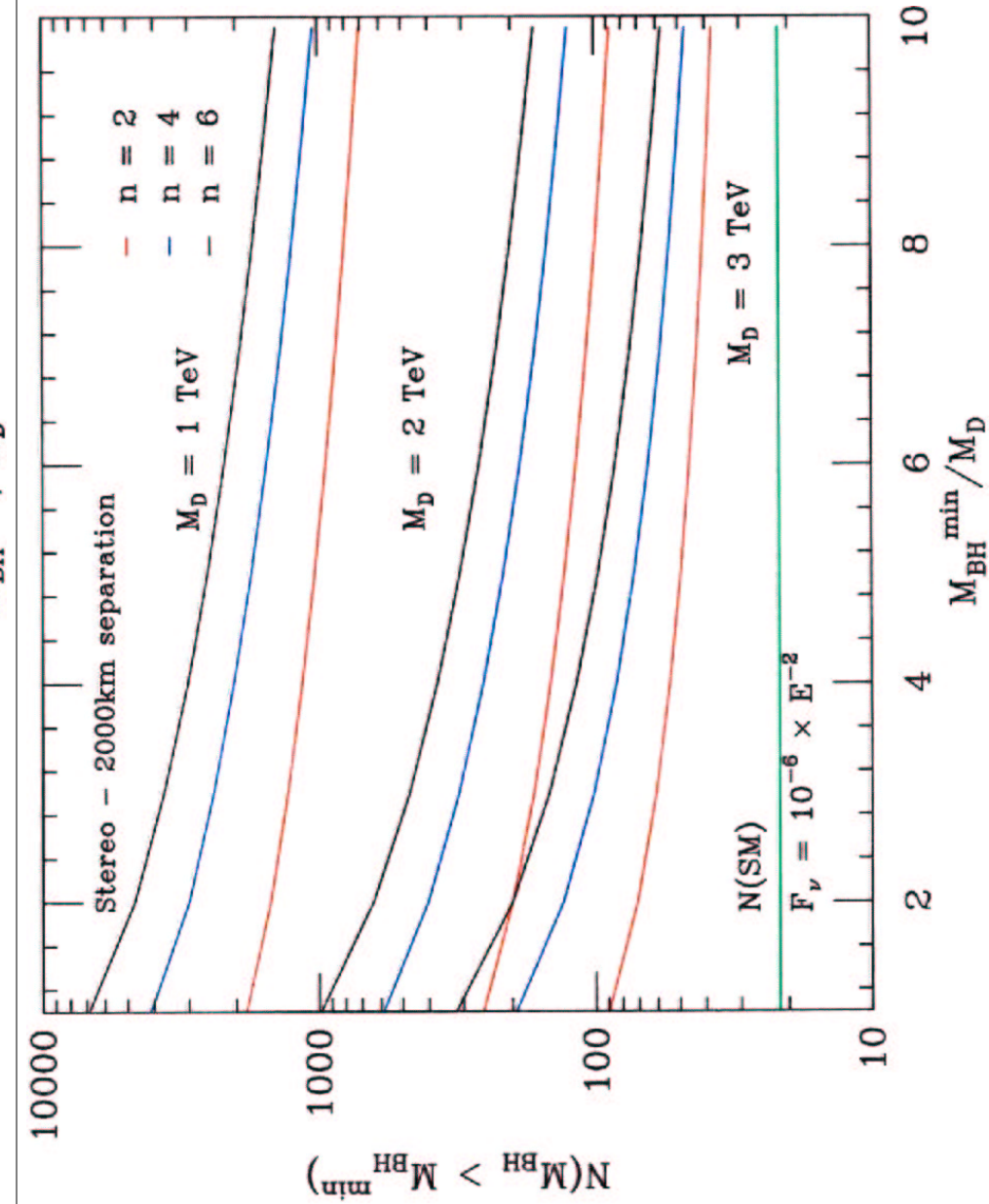
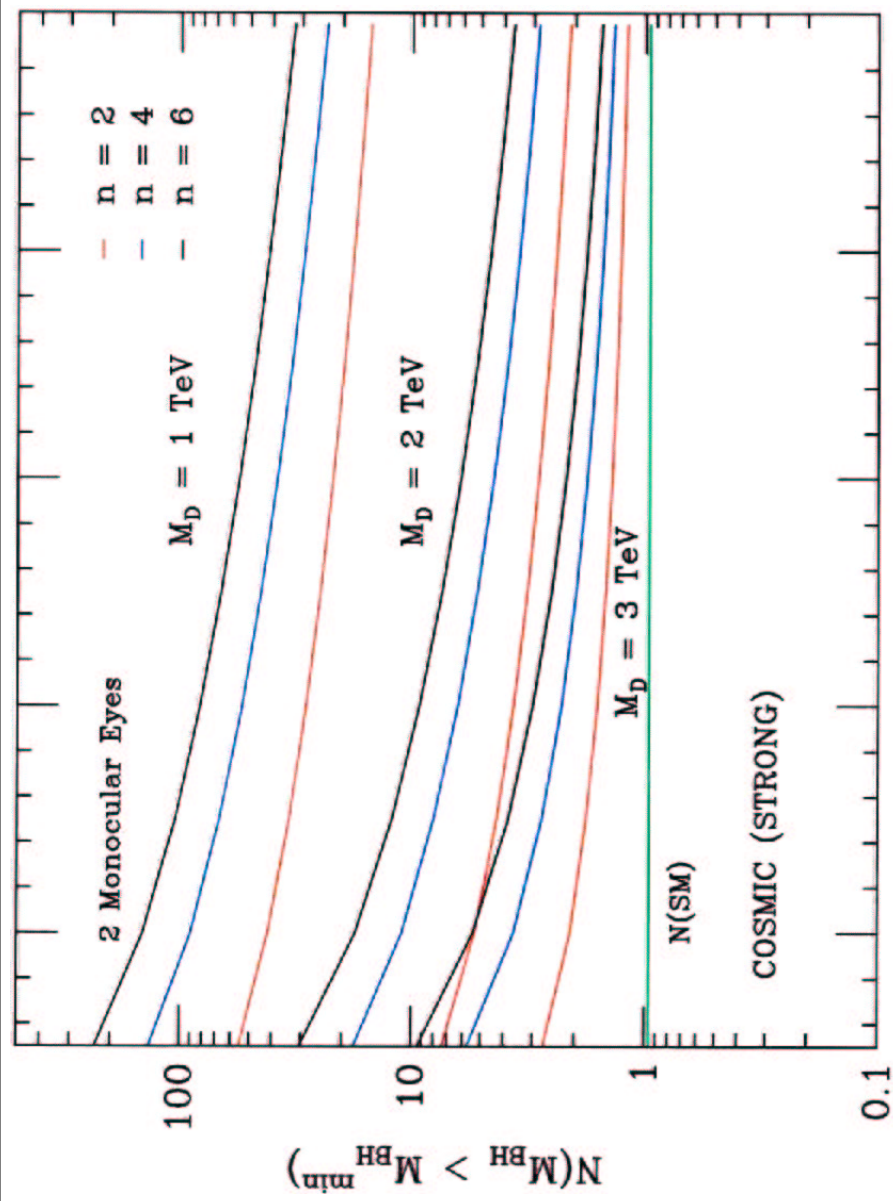


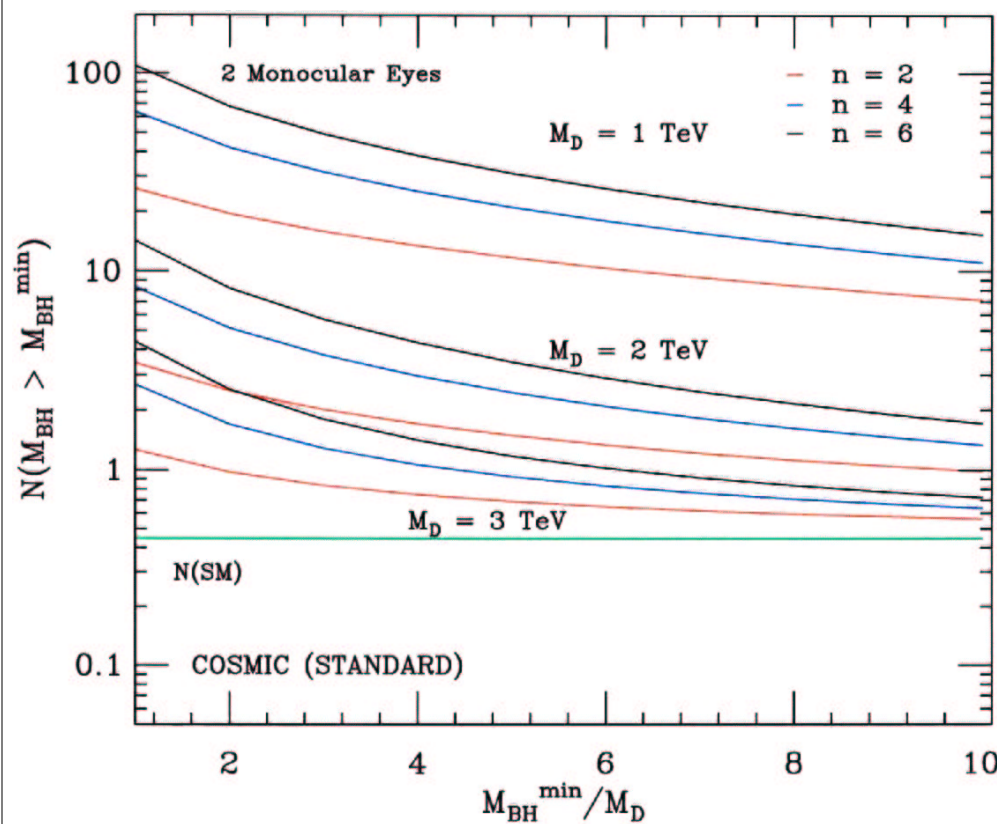
Gandhi et al., RHVS. REV D 58, 093009

OWL/AirWatch Neutrino Possibilities
UHE ν Workshop, November 1-4, 1999

John F. Krizmanic
USRA/NASA GSFC







Conclusion

- Kilometer-size neutrino telescope has a very good chance of detecting extragalactic neutrinos with energy threshold of 10TeV or 100TeV.
- Extragalactic neutrino sources, such as AGN, GRB and TD can provide 1000 megaparsec baseline for studying $\nu_\mu \rightarrow \nu_\tau$ oscillations.
- ν_τ upward flux is enhanced and has distinct angular and energy dependence at the detector.
- Detection of ν_τ appearance:
 - ★ Combined measurements of the upward muons and hadronic/em showers provide unambiguous signal of $\nu_\mu \rightarrow \nu_\tau$ oscillations independent of the theoretical uncertainties in the models of extragalactic neutrino sources.

- UHE neutrino interactions can probe physics scales above TeV \Rightarrow potential for discovering physics beyond the Standard Model.
- Production of black holes in νN interactions exceeds Standard Model cross section at energies above 10^8 GeV for $M_D \geq 2\text{TeV}$ and $n \geq 2$.
- Black Holes in Cosmic Rays: Limits from Fly's Eye and AGASSA, $M_D \approx 1\text{TeV} - 1.4\text{ TeV}$ excluded for $n \geq 4$. Pierre Auger experiment can probe $M_D \leq 2\text{ TeV}$ for any n .
- Black Holes with Neutrino Telescopes: ICECUBE rates for BH detection are promising for AGN and TD Models (for $M_D \leq 2\text{TeV}$, $n \geq 2$) but rates for cosmogenic neutrinos are too small.
- OWL could potentially probe the fundamental Planck scale up to $M_D = 3\text{TeV}$ for $n \geq 2$.